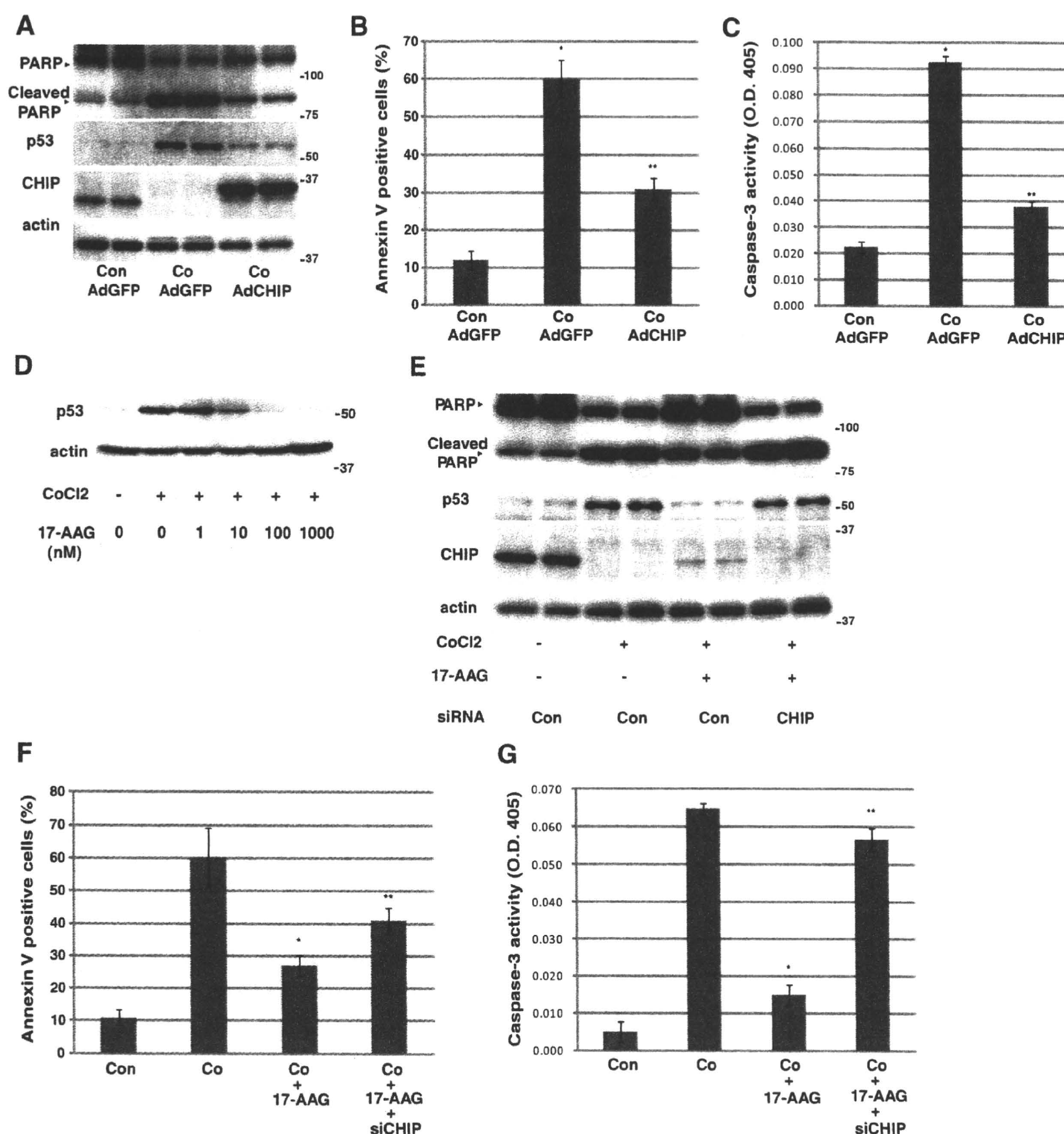

Figure 4. Promoting CHIP-mediated p53 degradation is protective against hypoxic stress. A through C, Overexpression of CHIP attenuates $CoCl_2$-induced p53 accumulation **(A)** and apoptosis in cardiomyocytes. Cardiomyocytes were infected with adenovirus harboring green fluorescent protein (GFP) or CHIP. Twenty-four hours later, culture medium was changed and the cells were treated with $CoCl_2$. Apoptosis was assessed by cleaved PARP expression **(A)**, Annexin V staining **(B)**, and caspase-3 activity **(C)**. *$P<0.01$ vs control (Con)+AdGFP; **$P<0.01$ vs Co+AdGFP; n=5. **D,** 17-AAG downregulates p53 expression in cardiomyocytes. Neonatal rat cardiomyocytes were treated with $CoCl_2$ with or without 17-AAG at the indicated concentration. **E through G,** 17-AAG inhibits $CoCl_2$-induced p53 accumulation **(E)** and apoptosis in cardiomyocytes, which is abrogated by CHIP knockdown. Neonatal rat cardiomyocytes were transfected with control siRNA or siRNA against CHIP. Twenty-four hours later, medium was changed and the cells were treated with $CoCl_2$ and/or 17-AAG. Apoptosis is assessed by cleaved PARP expression **(E)**, Annexin V staining **(F)**, and caspase-3 activity **(G)**. *$P<0.01$ vs Co; **$P<0.05$ vs Co +17-AAG; n=3.

We also examined whether treatment with 17-AAG exerts similar cardioprotective effects. 17-AAG (10 mg/kg) or vehicle was intraperitoneally injected immediately after permanent coronary artery ligation. This single injection of 17-AAG effectively suppressed the elevation of p53 protein levels and apoptotic cell death in the border zone of the infarct area at 24 hours after the operation (Figure 6A and 6B). As p53 protein level was kept elevated even 4 and 7 days after MI (Figure 2B), 17-AAG was injected every other days and we assessed whether 17-AAG treatment also leads to attenuation of ventricular remodeling, as observed in CHIP-Tg mice. At day 14, mice treated with 17-AAG exhibited smaller HW/BW ratio, better contractility,

Downloaded from circres.ahajournals.org at SWETS SUBS SERV-#25476254 on April 3, 2011

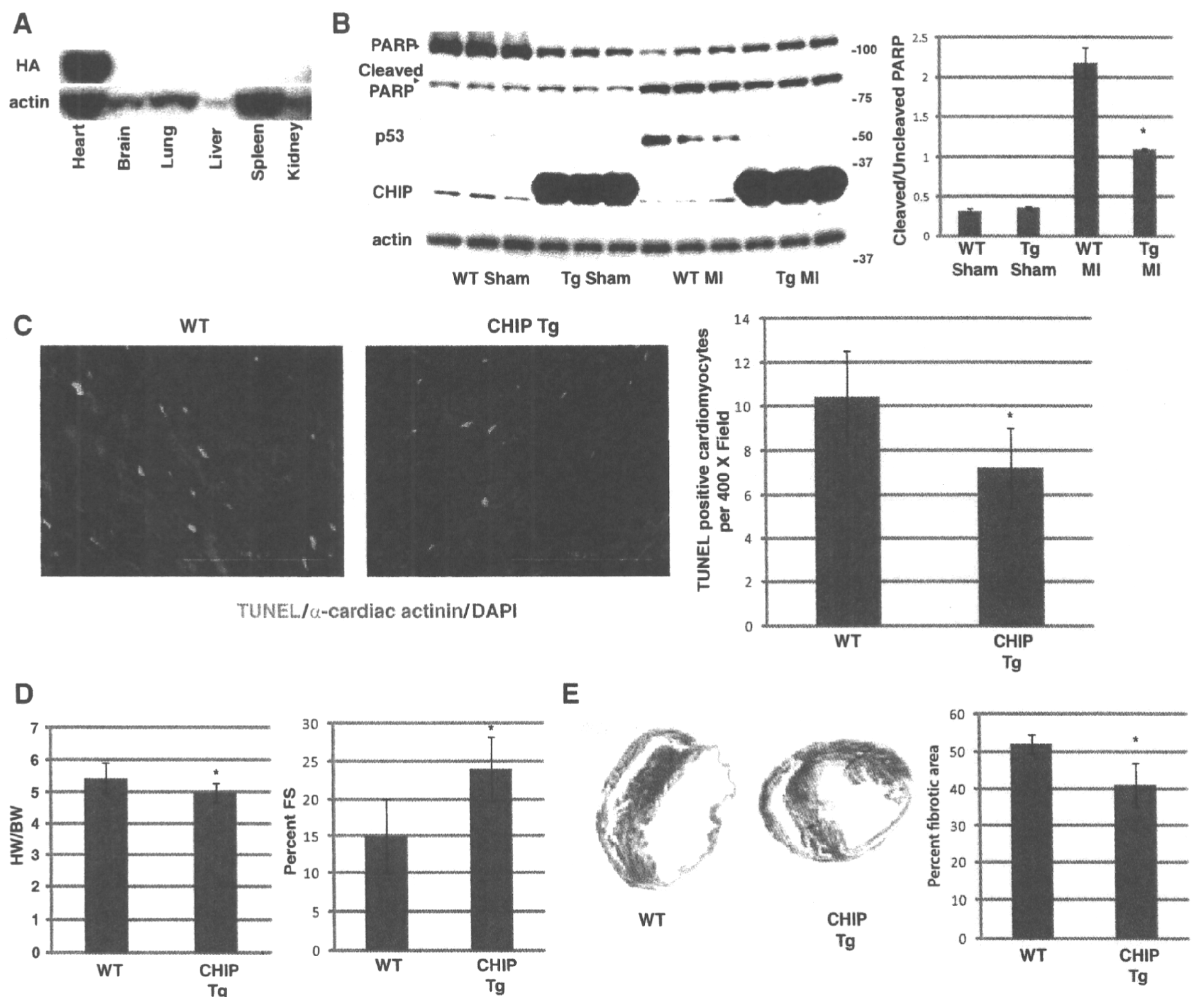

Figure 5. Overexpression of CHIP attenuates ischemic cardiac injury in vivo. A, Cardiac-specific expression of HA-tagged human CHIP in CHIP-Tg mice. **B and C,** p53 accumulation **(B)** and apoptosis 1 day after MI are reduced in CHIP-Tg mice. Apoptosis was assessed by cleaved PARP expression **(B)** and TUNEL staining **(C)**. Cleaved PARP level was assessed by densitometric analysis on band intensity of cleaved PARP over uncleaved PARP. $P<0.05$ vs WT; n=3. WT indicates wild-type mice. **D and E,** Postinfarct cardiac remodeling is attenuated in CHIP-Tg mice (n=15). HW/BW ratio **(D, left)**, contractile function **(D, right)**, and percentage fibrotic area **(E)**. *$P<0.01$ vs WT (n=30).

and less ventricular remodeling (Figure 6C and 6D). Interestingly, the effects of 17-AAG were greater than CHIP overexpression (compare Figures 5 and 6), suggesting that 17-AAG possesses cardioprotective activities that do not involve CHIP-mediated p53 degradation. As protein stability of cardioprotective proteins such as Hsp70 and HSF-1 was increased in vitro (Online Figure IV, B and C), we have examined the expression of these proteins in 17-AAG–treated mice. As expected, expression of these two proteins were increased by 17-AAG treatment (Online Figure IV, D), indicating that 17-AAG exerts its antiapoptotic effects by at least two mechanisms, one by inducing CHIP-mediated p53 degradation and the other by increasing cardioprotective heat shock proteins.

Finally, we examined the contribution of CHIP-mediated p53 degradation on the cardioprotective effects of 17-AAG. For that purpose we used CHIP heterozygous mice. There were no differences in cleaved PARP level (Figure 7A; compare WT Sham and Het Sham) or cardiac function between CHIP heterozygous mice and wild-type littermates at the basal level (Table). Following coronary artery ligation, however, apoptotic cell death was observed more prominently in CHIP heterozygous mice as assessed by increased cleaved PARP level (Figure 7A; compare WT MI and Het MI) and increased TUNEL positive cells (Figure 7B). The level of p53 accumulation was comparable following myocardial infarction between wild-type and CHIP heterozygous mice, suggesting the presence of p53 independent mechanisms for enhanced apoptosis caused by CHIP haploinsufficiency. Chronically, CHIP heterozygous mice showed worse cardiac function and worse ventricular remodeling compared with wild-type mice (Figure 7C and 7D). 17-AAG treatment was less effective to reduce p53 protein level, cleaved PARP level (Figure 7A; compare Het MI and Het MI 17-AAG), and TUNEL positive cardiomyocytes in CHIP heterozygous mice, possibly as a result of CHIP haploinsufficiency. 17-AAG treatment had minimal effects on improvements of cardiac function and ventricular remodeling on CHIP heterozygous mice also in the chronic phase (Figure 7C and 7D).

However, we must emphasize that the effects of 17-AAG were not fully attributable to CHIP-mediated p53 degradation

Downloaded from circres.ahajournals.org at SWETS SUBS SERV-#25476254 on April 3, 2011

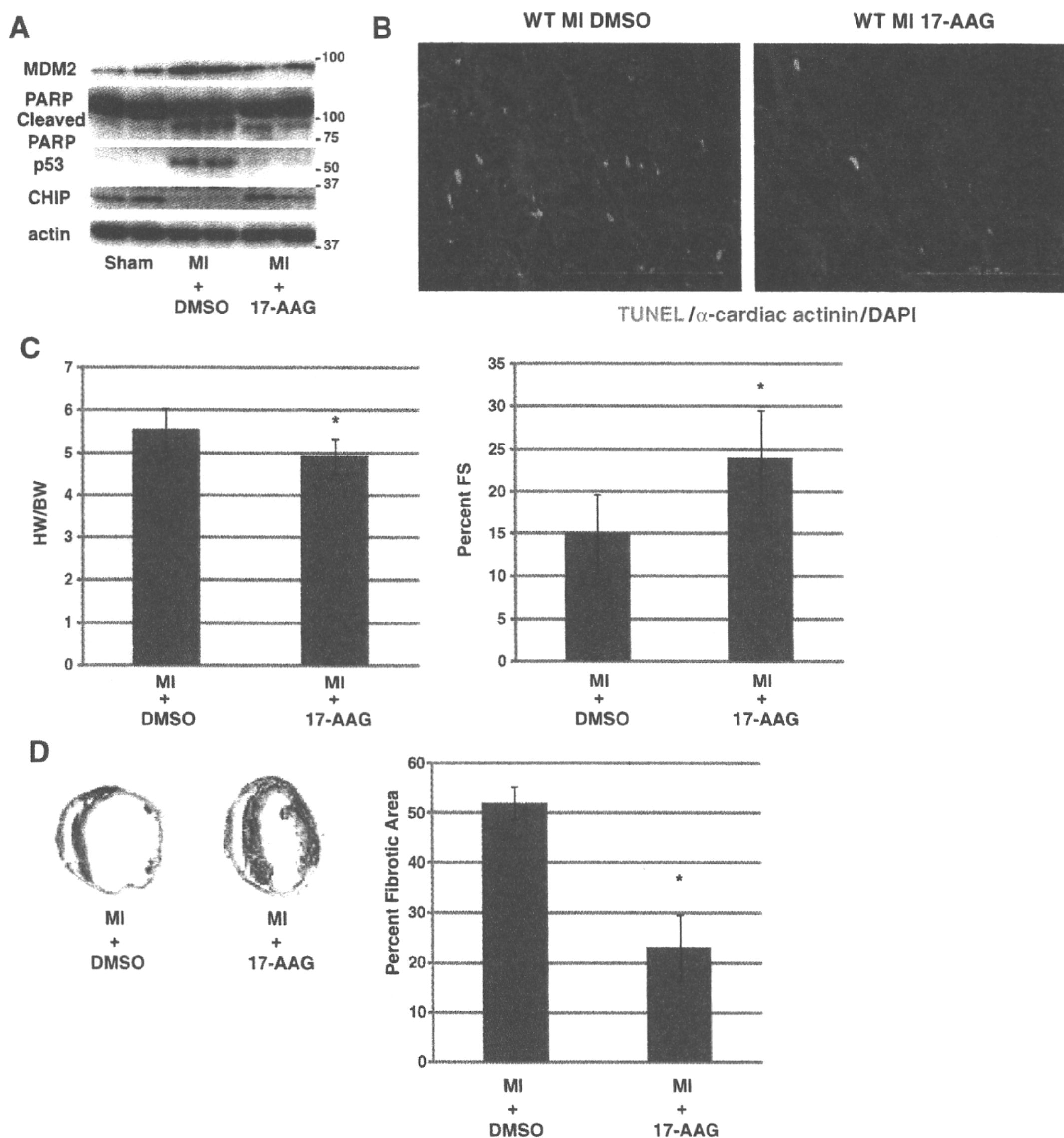

Figure 6. 17-AAG treatment attenuates ischemic cardiac injury in vivo. A, Accumulation of p53 and cleaved PARP in the heart after MI are reduced by 17-AAG treatment. 17-AAG (10 mg/kg) or vehicle was injected immediately after coronary ligation. **B,** Apoptotic cardiomyocytes at 1 day after MI was reduced in 17-AAG–treated mice. Apoptosis was assessed by TUNEL staining. **C and D,** Postinfarct cardiac remodeling is attenuated by 17-AAG treatment (n=20). HW/BW ratio **(C, left)**, contractile function **(C, right)**, and fibrotic area **(D)**. $^{*}P<0.001$; vs MI+DMSO (n=30).

because upregulation of heat shock proteins by 17-AAG was also impaired in CHIP heterozygous mice (Figure 7A; compare WT MI 17-AAG and Het MI 17-AAG). Therefore, it would be fair to conclude that 17-AAG exerts multiple cardioprotective effects after myocardial infarction and at least one of its effects were mediated by promotion of CHIP-mediated p53 degradation.

Discussion

In the present study, we found that accumulation of p53 protein after myocardial ischemia is initiated by HIF-1 dependent downregulation of CHIP level. We have found that CHIP overexpression decreased the amount of p53 and prevented myocardial apoptosis and ameliorated ventricular remodeling after myocardial infarction. We have also found that Hsp90 inhibitor, 17-AAG, exerted similar antiapoptotic and cardioprotective effects after myocardial infarction and showed that these effects of 17-AAG was at least in part mediated by promotion of CHIP-mediated p53 degradation.

Although hypoxic stimuli have been reported to raise p53 protein levels in a variety of cell types, molecular mechanisms of p53 accumulation have been largely unknown. In the present study, we unveiled that downregulation of CHIP protein is critically involved in this process. We found that CHIP expression was downregulated after hypoxic stress through HIF-1–mediated suppression of *CHIP* promoter (Figure 2). We also found that overexpression of CHIP attenuated the p53 accumulation after hypoxic stress (Figures 4A and 5B). These results

Downloaded from circres.ahajournals.org at SWETS SUBS SERV-#25476254 on April 3, 2011

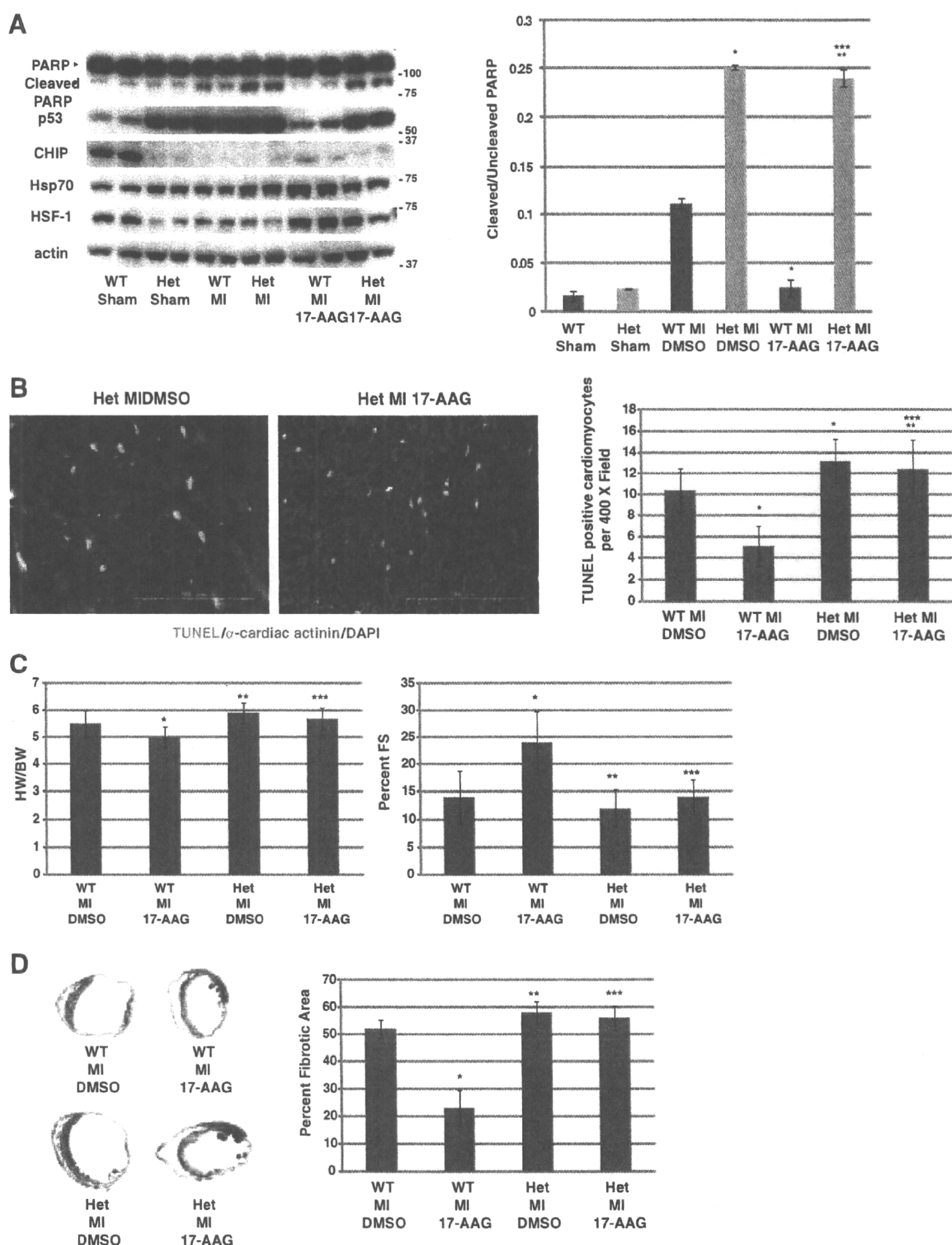

Figure 7. The effect of 17-AAG was dependent on CHIP-mediated p53 degradation and upregulation of heat shock proteins. A, 17-AAG–induced reduction of p53 accumulation and PARP expression was not observed in the heart of CHIP heterozygous mice (Het). Notably, upregulation of heat shock proteins by 17-AAG was ameliorated in CHIP heterozygous mice. **B,** Apoptotic cardiomyocytes on 1 day after MI was reduced in 17-AAG–treated mice, but this antiapoptotic effect of 17-AAG after MI was ameliorated in CHIP heterozygous mice. Apoptosis was assessed by cleaved PARP expression **(A)** and TUNEL staining **(B)**. *$P<0.01$ vs WT+MI+DMSO; **$P<0.01$ vs WT+MI +17-AAG; ***P=NS vs Het+MI+DMSO n=5. WT indicates wild-type mice; Het, CHIP heterozygous mice. **C,** 17-AAG–induced attenuation of postinfarct cardiac remodeling is less in CHIP hetero knockout mice than in wild-type mice. HW/BW ratio **(C, left)**, contractile function **(C, right)**, and fibrotic area **(D)**. *$P<0.001$; **$P<0.05$ vs WT+MI+DMSO; ***P=NS vs Het+MI+DMSO. WT+MI+DMSO: n=30; WT+MI +17-AAG: n=20; Het+MI+DMSO: n=15; Het+MI +17-AAG: n=15. WT indicates wild-type mice.

Downloaded from circres.ahajournals.org at SWETS SUBS SERV-#25476254 on April 3, 2011

Table. Basal Characterization of the Mice Used in this Study

	Body Weight (g)	LVEDD (mm)	LVESD (mm)	IVS (mm)	LVPW (mm)	%FS
Wild type	26.3±1.2	3.12±0.12	1.04±0.02	0.72±0.02	0.74±0.02	66.7±1.3
CHIP hetero KO	25.6±0.8	3.10±0.08	1.05±0.03	0.74±0.03	0.78±0.02	66.1±0.8
CHIP Tg	26.9±1.5	3.14±0.16	1.05±0.04	0.75±0.02	0.75±0.05	66.6±1.8

suggest that hypoxic stress downregulates CHIP, leading to decreased CHIP-mediated proteolysis of p53 protein and accumulation of p53 protein. This mechanism seems to be a 'fine-tuning' of HIF-1 activity because p53 protein has been reported to bind to and inhibit HIF-1 activity.[16] After hypoxia, first HIF-1 accumulates and induces angiogenic genes, to promote angiogenesis. Thereafter, as a negative feedback loop, HIF-1 induces downregulation of *CHIP* expression and p53 accumulates, then accumulated p53 inhibits HIF-1 activity.[35] In general, this feedback system might have an antitumor effect, because in many tumor cells HIF-1 induces feeding vessels in hypoxic tumors and promotes tumor growth. HIF-1-induced, CHIP-mediated p53 accumulation acts to suppress tumor growth by (1) suppressing HIF-1 activity and blocking neovascularization and (2) inducing p53-mediated apoptosis of tumor cells. However, in the heart, this negative feedback system worsens hypoxic situation by blocking neovascularization[16] and by inducing apoptosis (this study).

The important role of apoptosis in the progression of ventricular remodeling and the possibility of antiapoptotic approach against heart failure has already been elegantly shown by Wencker et al.[3] Antiapoptotic approach after myocardial infarction has been reported to be cardioprotective not only in ischemia-reperfusion model but also in permanent coronary ligation model.[21,36,37] Therefore, inhibition of apoptotic death does not only reduce initial infarct size but also prevents ventricular remodeling through inhibiting apoptosis in the border zone of the infarct.

Accumulation of p53 has been reported to initiate many proapoptotic triggers.[38] In the heart, p53 accumulates (Figure 3C) and p53-dependent apoptosis occurs[39] after permanent coronary occlusion. We have also observed that *p53* gene deletion lead to less ventricular remodeling after myocardial infarction.[16] In the present study, we have shown that CHIP overexpression or 17-AAG treatment could prevent cardiomyocyte apoptosis and ameliorate ventricular remodeling after myocardial infarction. We have also shown some evidences that inhibition of p53 accumulation is at least one of the mechanisms for the effect of CHIP overexpression and 17-AAG. However, it should be noted that Hsp90 chaperones various proteins including prosurvival factors such as Akt/protein kinase B[40] in tumor cells and that Hsp90 inhibitors induced degradation of aberrantly overexpressed prosurvival factors in those tumor cells. Although the nature of the effects of 17-AAG seems to induce degradation of aberrantly expressed proteins, it is also possible and taken into account that 17-AAG could also induce degradation of prosurvival factors and play detrimental effects in cardiomyocytes.

In conclusion, our observations indicate that investigation of novel anti-p53 approach would open a way toward new treatment of myocardial infarction.

Acknowledgments

We thank Y. Ohtsuki, I. Sakamoto, M. Ikeda, and A. Furuyama for excellent technical support.

Sources of Funding

This work was supported by a Grant-in-Aid for Scientific Research on Priority Areas and for Exploratory Research (Ministry of Education, Culture, Sports, Science and Technology), Health and Labour Sciences Research grants (to I.K.), and research fellowships from the Japan Society for the Promotion of Science for Young Scientists (to A.T.N.). A.T.N. is a research fellow of the Japan Society for the Promotion of Science.

Disclosures

None.

References

1. Rosamond W, Flegal K, Friday G, Furie K, Go A, Greenlund K, Haase N, Ho M, Howard V, Kissela B, Kittner S, Lloyd-Jones D, McDermott M, Meigs J, Moy C, Nichol G, O'Donnell CJ, Roger V, Rumsfeld J, Sorlie P, Steinberger J, Thom T, Wasserthiel-Smoller S, Hong Y. Heart disease and stroke statistics–2007 update: a report from the American Heart Association Statistics Committee and Stroke Statistics Subcommittee. *Circulation*. 2007;115:e69–e171.
2. Kajstura J, Cheng W, Reiss K, Clark WA, Sonnenblick EH, Krajewski S, Reed JC, Olivetti G, Anversa P. Apoptotic and necrotic myocyte cell deaths are independent contributing variables of infarct size in rats. *Lab Invest*. 1996;74:86–107.
3. Wencker D, Chandra M, Nguyen K, Miao W, Garantziotis S, Factor SM, Shirani J, Armstrong RC, Kitsis RN. A mechanistic role for cardiac myocyte apoptosis in heart failure. *J Clin Invest*. 2003;111:1497–1504.
4. Haunstetter A, Izumo S. Toward antiapoptosis as a new treatment modality. *Circ Res*. 2000;86:371–376.
5. Chatterjee S, Stewart AS, Bish LT, Jayasankar V, Kim EM, Pirolli T, Burdick J, Woo YJ, Gardner TJ, Sweeney HL. Viral gene transfer of the antiapoptotic factor Bcl-2 protects against chronic postischemic heart failure. *Circulation*. 2002;106:I212–I217.
6. Hochhauser E, Kivity S, Offen D, Maulik N, Otani H, Barhum Y, Pannet H, Shneyvays V, Shainberg A, Goldshtaub V, Tobar A, Vidne BA. Bax ablation protects against myocardial ischemia-reperfusion injury in transgenic mice. *Am J Physiol Heart Circ Physiol*. 2003;284:H2351–H2359.
7. Imahashi K, Schneider MD, Steenbergen C, Murphy E. Transgenic expression of Bcl-2 modulates energy metabolism, prevents cytosolic acidification during ischemia, and reduces ischemia/reperfusion injury. *Circ Res*. 2004;95:734–741.
8. Hochhauser E, Cheporko Y, Yasovich N, Pinchas L, Offen D, Barhum Y, Pannet H, Tobar A, Vidne BA, Birk E. Bax deficiency reduces infarct size and improves long-term function after myocardial infarction. *Cell Biochem Biophys*. 2007;47:11–20.
9. Vogelstein B, Lane D, Levine AJ. Surfing the p53 network. *Nature*. 2000;408:307–310.
10. Haupt Y, Maya R, Kazaz A, Oren M. Mdm2 promotes the rapid degradation of p53. *Nature*. 1997;387:296–299.
11. Kubbutat MH, Jones SN, Vousden KH. Regulation of p53 stability by Mdm2. *Nature*. 1997;387:299–303.
12. Dornan D, Wertz I, Shimizu H, Arnott D, Frantz GD, Dowd P, O'Rourke K, Koeppen H, Dixit VM. The ubiquitin ligase COP1 is a critical negative regulator of p53. *Nature*. 2004;429:86–92.
13. Leng RP, Lin Y, Ma W, Wu H, Lemmers B, Chung S, Parant JM, Lozano G, Hakem R, Benchimol S. Pirh2, a p53-induced ubiquitin-protein ligase, promotes p53 degradation. *Cell*. 2003;112:779–791.
14. Long X, Boluyt MO, Hipolito ML, Lundberg MS, Zheng JS, O'Neill L, Cirielli C, Lakatta EG, Crow MT. p53 and the hypoxia-induced apoptosis

Downloaded from circres.ahajournals.org at SWETS SUBS SERV-#25476254 on April 3, 2011

of cultured neonatal rat cardiac myocytes. *J Clin Invest*. 1997;99: 2635–2643.
15. Liu P, Xu B, Cavalieri TA, Hock CE. Pifithrin-alpha attenuates p53-mediated apoptosis and improves cardiac function in response to myocardial ischemia/reperfusion in aged rats. *Shock*. 2006;26:608–614.
16. Sano M, Minamino T, Toko H, Miyauchi H, Orimo M, Qin Y, Akazawa H, Tateno K, Kayama Y, Harada M, Shimizu I, Asahara T, Hamada H, Tomita S, Molkentin JD, Zou Y, Komuro I. p53-induced inhibition of Hif-1 causes cardiac dysfunction during pressure overload. *Nature*. 2007; 446:444–448.
17. Song K, Backs J, McAnally J, Qi X, Gerard RD, Richardson JA, Hill JA, Bassel-Duby R, Olson EN. The transcriptional coactivator CAMTA2 stimulates cardiac growth by opposing class II histone deacetylases. *Cell*. 2006;125:453–466.
18. Zou Y, Komuro I, Yamazaki T, Kudoh S, Uozumi H, Kadowaki T, Yazaki Y. Both Gs and Gi proteins are critically involved in isoproterenol-induced cardiomyocyte hypertrophy. *J Biol Chem*. 1999;274:9760–9770.
19. Sohal DS, Nghiem M, Crackower MA, Witt SA, Kimball TR, Tymitz KM, Penninger JM, Molkentin JD. Temporally regulated and tissue-specific gene manipulations in the adult and embryonic heart using a tamoxifen-inducible Cre protein. *Circ Res*. 2001;89:20–25.
20. Sahara N, Murayama M, Mizoroki T, Urushitani M, Imai Y, Takahashi R, Murata S, Tanaka K, Takashima A. In vivo evidence of CHIP up-regulation attenuating tau aggregation. *J Neurochem*. 2005;94:1254–1263.
21. Harada M, Qin Y, Takano H, Minamino T, Zou Y, Toko H, Ohtsuka M, Matsuura K, Sano M, Nishi J, Iwanaga K, Akazawa H, Kunieda T, Zhu W, Hasegawa H, Kunisada K, Nagai T, Nakaya H, Yamauchi-Takihara K, Komuro I. G-CSF prevents cardiac remodeling after myocardial infarction by activating the Jak-Stat pathway in cardiomyocytes. *Nat Med*. 2005;11:305–311.
22. McDonough H, Patterson C. CHIP: a link between the chaperone and proteasome systems. *Cell Stress Chaperones*. 2003;8:303–308.
23. Esser C, Scheffner M, Hohfeld J. The chaperone-associated ubiquitin ligase CHIP is able to target p53 for proteasomal degradation. *J Biol Chem*. 2005;280:27443–27448.
24. Tripathi V, Ali A, Bhat R, Pati U. CHIP chaperones wild type p53 tumor suppressor protein. *J Biol Chem*. 2007;282:28441–28454.
25. Graeber TG, Peterson JF, Tsai M, Monica K, Fornace AJ Jr, Giaccia AJ. Hypoxia induces accumulation of p53 protein, but activation of a G1-phase checkpoint by low-oxygen conditions is independent of p53 status. *Mol Cell Biol*. 1994;14:6264–6277.
26. An WG, Kanekal M, Simon MC, Maltepe E, Blagosklonny MV, Neckers LM. Stabilization of wild-type p53 by hypoxia-inducible factor 1alpha. *Nature*. 1998;392:405–408.
27. Chen KF, Lai YY, Sun HS, Tsai SJ. Transcriptional repression of human cad gene by hypoxia inducible factor-1alpha. *Nucleic Acids Res*. 2005; 33:5190–5198.
28. Eltzschig HK, Abdulla P, Hoffman E, Hamilton KE, Daniels D, Schonfeld C, Loffler M, Reyes G, Duszenko M, Karhausen J, Robinson A, Westerman KA, Coe IR, Colgan SP. HIF-1-dependent repression of equilibrative nucleoside transporter (ENT) in hypoxia. *J Exp Med*. 2005;202:1493–1505.
29. Ibla JC, Khoury J, Kong T, Robinson A, Colgan SP. Transcriptional repression of Na-K-2Cl cotransporter NKCC1 by hypoxia-inducible factor-1. *Am J Physiol Cell Physiol*. 2006;291:C282–C289.
30. Bindra RS, Glazer PM. Co-repression of mismatch repair gene expression by hypoxia in cancer cells: role of the Myc/Max network. *Cancer Lett*. 2007;252:93–103.
31. Waza M, Adachi H, Katsuno M, Minamiyama M, Sang C, Tanaka F, Inukai A, Doyu M, Sobue G. 17-AAG, an Hsp90 inhibitor, ameliorates polyglutamine-mediated motor neuron degeneration. *Nat Med*. 2005;11: 1088–1095.
32. Dickey CA, Kamal A, Lundgren K, Klosak N, Bailey RM, Dunmore J, Ash P, Shoraka S, Zlatkovic J, Eckman CB, Patterson C, Dickson DW, Nahman NS Jr, Hutton M, Burrows F, Petrucelli L. The high-affinity HSP90-CHIP complex recognizes and selectively degrades phosphorylated tau client proteins. *J Clin Invest*. 2007;117:648–658.
33. Suzuki K, Sawa Y, Kaneda Y, Ichikawa H, Shirakura R, Matsuda H. In vivo gene transfection with heat shock protein 70 enhances myocardial tolerance to ischemia-reperfusion injury in rat. *J Clin Invest*. 1997;99:1645–1650.
34. Sakamoto M, Minamino T, Toko H, Kayama Y, Zou Y, Sano M, Takaki E, Aoyagi T, Tojo K, Tajima N, Nakai A, Aburatani H, Komuro I. Upregulation of heat shock transcription factor 1 plays a critical role in adaptive cardiac hypertrophy. *Circ Res*. 2006;99:1411–1418.
35. Blagosklonny MV, An WG, Romanova LY, Trepel J, Fojo T, Neckers L. p53 inhibits hypoxia-inducible factor-stimulated transcription. *J Biol Chem*. 1998;273:11995–11998.
36. Chandrashekhar Y, Sen S, Anway R, Shuros A, Anand I. Long-term caspase inhibition ameliorates apoptosis, reduces myocardial troponin-I cleavage, protects left ventricular function, and attenuates remodeling in rats with myocardial infarction. *J Am Coll Cardiol*. 2004;43:295–301.
37. Balsam LB, Kofidis T, Robbins RC. Caspase-3 inhibition preserves myocardial geometry and long-term function after infarction. *J Surg Res*. 2005;124:194–200.
38. Crow MT, Mani K, Nam YJ, Kitsis RN. The mitochondrial death pathway and cardiac myocyte apoptosis. *Circ Res*. 2004;95:957–970.
39. Matsusaka H, Ide T, Matsushima S, Ikeuchi M, Kubota T, Sunagawa K, Kinugawa S, Tsutsui H. Targeted deletion of p53 prevents cardiac rupture after myocardial infarction in mice. *Cardiovasc Res*. 2006;70: 457–465.
40. Solit DB, Basso AD, Olshen AB, Scher HI, Rosen N. Inhibition of heat shock protein 90 function downregulates Akt kinase and sensitizes tumors to Taxol. *Cancer Res*. 2003;63:2139–2144.

Novelty and Significance

What Is Known?

- Inhibition of myocardial apoptosis after myocardial infarction is cardioprotective.
- p53 expression is increased after myocardial infarction and induces cardiomyocyte apoptosis.

What New Information Does This Article Contribute?

- We identified CHIP as the endogenous p53 antagonist expressed in the heart.
- We found that CHIP downregulation is critically involved in the molecular mechanisms for p53 elevation after myocardial infarction.
- We showed several possibilities of the anti-p53 treatment after myocardial infarction.

Accumulation of tumor suppressor protein p53 in the myocardium causes the transition from adaptive cardiac hypertrophy to heart failure. However, the mechanisms of p53 accumulation in the heart and its therapeutic implications have been elusive. Here we show that downregulation of the chaperone-associated E3 ubiquitin ligase CHIP (carboxyl terminus of Hsp70-interacting protein) mediates hypoxia-induced p53 accumulation in the heart and that promotion of CHIP-induced p53 degradation protects the heart from ischemic injury. Under physiological conditions, CHIP limited the p53 protein amount at low levels by inducing proteasomal degradation of p53. Under hypoxic conditions, hypoxia inducible factor-1 (HIF-1) down-regulated CHIP, resulting in the accumulation of p53. Overexpression of CHIP or administration of an Hsp90 inhibitor promoted CHIP-mediated p53 degradation and attenuated ischemic cardiac injury. These results indicate that CHIP is a crucial negative regulator of p53 in the heart and suggest that promotion of CHIP-mediated p53 degradation could be a novel therapeutic strategy for heart diseases.

Downloaded from circres.ahajournals.org at SWETS SUBS SERV-#25476254 on April 3, 2011

Ca^{2+}/Calmodulin-Dependent Kinase IIδ Causes Heart Failure by Accumulation of p53 in Dilated Cardiomyopathy

Haruhiro Toko, MD, PhD; Hidehisa Takahashi, MD, PhD; Yosuke Kayama, MD; Toru Oka, MD, PhD; Tohru Minamino, MD, PhD; Sho Okada, MD, PhD; Sachio Morimoto, PhD; Dong-Yun Zhan, PhD; Fumio Terasaki, MD, PhD; Mark E. Anderson, MD, PhD; Masashi Inoue, MD, PhD; Atsushi Yao, MD, PhD; Ryozo Nagai, MD, PhD; Yasushi Kitaura, MD, PhD; Toshiyuki Sasaguri, MD, PhD; Issei Komuro, MD, PhD

Background—Dilated cardiomyopathy (DCM), characterized by dilatation and dysfunction of the left ventricle, is an important cause of heart failure. Many mutations in various genes, including cytoskeletal protein genes and contractile protein genes, have been identified in DCM patients, but the mechanisms of how such mutations lead to DCM remain unknown.

Methods and Results—We established the mouse model of DCM by expressing a mutated cardiac α-actin gene, which has been reported in patients with DCM, in the heart (mActin-Tg). mActin-Tg mice showed gradual dilatation and dysfunction of the left ventricle, resulting in death by heart failure. The number of apoptotic cardiomyocytes and protein levels of p53 were increased in the hearts of mActin-Tg mice. Overexpression of Bcl-2 or downregulation of p53 decreased the number of apoptotic cardiomyocytes and improved cardiac function. This mouse model showed a decrease in myofilament calcium sensitivity and activation of calcium/calmodulin-dependent kinase IIδ (CaMKIIδ). The inhibition of CaMKIIδ prevented the increase in p53 and apoptotic cardiomyocytes and ameliorated cardiac function.

Conclusion—CaMKIIδ plays a critical role in the development of heart failure in part by accumulation of p53 and induction of cardiomyocyte apoptosis in the DCM mouse model. **(*Circulation*. 2010;122:891-899.)**

Key Words: apoptosis ■ CaMKII ■ cardiomyopathy ■ heart failure ■ genes, p53

Heart failure is an important cause of morbidity and mortality in many industrial countries, and dilated cardiomyopathy (DCM) is one of its major causes.[1] Although treatments for heart failure have been progressed well in both pharmacological and nonpharmacological aspects, mortality of DCM patients remains high, and the only treatment for DCM patients with severe symptoms is heart transplantation. Because the number of hearts for transplantation is limited, the development of novel therapies for DCM has been awaited.

Clinical Perspective on p 899

DCM, characterized by dilatation and impaired contraction of the left ventricle, is a multifactorial disease that includes both hereditary and acquired forms. The acquired forms of DCM are caused by various factors.[2] Twenty percent to 35% of patients have hereditary forms,[1] and advances in molecular genetic studies during the last decade have revealed many mutations of various genes in DCM patients.[3–5]

Several hypotheses have been reported on the mechanisms of how gene mutations lead to DCM phenotypes. Mutations in genes encoding cytoskeletal proteins such as desmin and muscle LIM protein might disturb the interaction between the sarcomere and Z disk, resulting in impaired force transmission from the sarcomere to the surrounding syncytium.[4,6] On the other hand, mutations in genes encoding contractile proteins such as α-tropomyosin and cardiac troponin T have been reported to induce the decrease in myofilament calcium (Ca^{2+}) sensitivity.[7] An increase in apoptotic cardiomyocytes and/or destruction of membrane structure by calpain activa-

Received January 6, 2010; accepted July 2, 2010.
From the Department of Cardiovascular Science and Medicine, Chiba University Graduate School of Medicine, Chiba, Japan (H. Toko, H. Takahashi, Y.K., T.O., T.M., S.O., I.K.); Department of Cardiovascular Medicine, Osaka University Graduate School of Medicine, Suita, Japan (T.O., I.K.); Department of Clinical Pharmacology, Kyusyu University Graduate School of Medicine, Fukuoka, Japan (S.M., D.Z., T.S.); Department of Internal Medicine III, Osaka Medical College, Takatsuki, Japan (F.T., Y.K.); Department of Internal Medicine, and Molecular Physiology and Biophysics, Carver College of Medicine, University of Iowa, Iowa City (M.E.A.); and Department of Cardiovascular Medicine, University of Tokyo Graduate School of Medicine, Tokyo, Japan (M.I., A.Y., R.N.).
The online-only Data Supplement is available with this article at http://circ.ahajournals.org/cgi/content/full/CIRCULATIONAHA.109.935296/DC1.
Correspondence to Issei Komuro, MD, PhD, Department of Cardiovascular Medicine, Osaka University Graduate School of Medicine, 2-2 Yamadaoka, Suita 565-0871, Japan. E-mail komuro-tky@umin.ac.jp
© 2010 American Heart Association, Inc.

***Circulation* is available at http://circ.ahajournals.org** **DOI: 10.1161/CIRCULATIONAHA.109.935296**

tion have been reported to play a critical role in mutant gene–induced cardiac dysfunction.[8–10] However, the precise mechanisms remain largely unknown as a result, at least in part, of a lack of good animal models of DCM.

Several animal models of DCM have been reported.[11–13] The *mdx* mouse is a model of Duchenne muscular dystrophy, which has mutations in the dystrophin gene.[11] Unlike humans, *mdx* mice rarely show cardiac abnormality, which has limited the utility of *mdx* mice as a model to examine the pathogenesis of DCM. Although Golden Retriever–based muscular dystrophy dogs show DCM phenotypes,[12] the muscular dystrophy dogs are very difficult to maintain and handle. Although BIO 14.6 hamsters lacking δ-sarcoglycan are a good model of DCM,[13] it is difficult to apply genetic approaches to the hamster. To elucidate the molecular mechanisms of how gene mutations cause DCM, appropriate animal models, particularly mouse models, are necessary. We established here a mouse model of DCM by expressing a mutated cardiac α-actin gene (mActin-Tg), which has been reported in patients with DCM, in the heart.[5] mActin-Tg mice showed gradual dilatation and dysfunction of the left ventricle, resulting in death by heart failure. These phenotypes of mActin-Tg mice were quite similar to those of human DCM. In this study, we examined the underlying mechanisms of how this gene mutation leads to DCM using the new mouse model of DCM.

Methods

Detailed experimental methods are described in the online-only Data Supplement.

Mice

We generated transgenic mice (mActin-Tg) that expressed a mutated cardiac α-actin (R312H) with an HA tag in the heart. This mutation has been reported in patients with DCM.[5] Generation of transgenic mice with cardiac-restricted overexpression of human Bcl-2, AC3-I, or nuclear factor of activated T cell (NFAT)–luciferase has been described previously.[14–16] Heterozygous p53-deficient mice were purchased from The Jackson Laboratory (Bar Harbor, Me).[17] Wild-type littermates served as controls for all studies. KN-93 (10 μmol · kg^{-1} · $/d^{-1}$) was used to inhibit activation of Ca^{2+}/calmodulin-dependent kinase II (CaMKII). Echocardiography was performed on conscious mice.

Histology

For detection of apoptotic cardiomyocytes, we performed terminal deoxynucleotidyl transferase–mediated dUTP nick-end labeling (TUNEL) staining, along with immunostaining for dystrophin.

Western Blot Analysis

Whole-cell lysates were resolved by SDS-PAGE. Western blot analyses were performed with some antibodies. The intensities of Western blot bands were measured with NIH ImageJ software (National Institutes of Health, Bethesda, Md).

Luciferase Assay

Left ventricles were homogenized in luciferase assay buffer as described previously.[15]

Force Measurements

A small fiber was dissected from the skinned left ventricular papillary muscle, and isometric force was measured as described previously.[7]

RNA Extraction and Quantitative Real-Time Polymerase Chain Reaction Analysis

Quantitative real-time polymerase chain reaction was performed with the LightCycler with the Taqman Universal Probe Library and Light Cycler Master. Relative levels of gene expressions were normalized to the mouse GAPDH expression with the ΔΔCt method.[18]

Statistical Analysis

Data are shown as mean±SEM. Multiple-group comparison was performed by 1-way ANOVA followed by the Bonferroni procedure for comparison of means. The F test was used to assess equal variances before comparison between 2 groups. Then, comparisons between 2 groups were performed with the Student t test (when $P>0.05$ in the F test) and the Welch t test (when $P<0.05$ in the F test). Survival rates were analyzed with the log-rank test. Values of $P<0.05$ were considered statistically significant.

Results

DCM Model Mouse

Because there are few useful DCM mouse models, we first generated transgenic mice that expressed a cardiac α-actin R312H mutant with an HA tag under the control of α-myosin heavy chain promoter (mActin-Tg). We obtained 3 independent founders of the transgenic mice (lines 301, 307, and 311). The protein levels of the cardiac α-actin R312H mutant were 1.6-fold in line 301, 3.3-fold in line 307, and 2.2-fold in line 311 compared with those of endogenous cardiac α-actin (Figure IA in the online-only Data Supplement). To confirm the expression of the transgene in cardiomyocytes, we performed immunohistological analyses with antibodies against HA and actinin. The mutated cardiac α-actin protein was colocalized with actinin, suggesting that the cardiac α-actin R312H mutant is incorporated into myofilaments (Figure IB in the online-only Data Supplement). Cardiac systolic function was decreased in mActin-Tg mice at 10 months of age, and the reduction was well correlated with protein levels of the cardiac α-actin R312H mutant (Figure IC in the online-only Data Supplement). To further investigate whether cardiac expression of the cardiac α-actin R312H mutant led to heart failure, we examined another transgenic mouse that expressed cardiac α-actin A331P mutant with an HA tag in the heart. This mutant has been reported to cause hypertrophic cardiomyopathy in human.[19] We obtained 2 independent founders of the transgenic mice that expressed almost the same levels of the cardiac α-actin A331P mutant protein. Although the protein levels of the mutant in the A331P mutant transgenic mice were almost same as those of the R312H mutant in line 307, which had the highest expression (Figure II in the online-only Data Supplement), echocardiography revealed that there were no significant differences in cardiac systolic function, wall thickness, and left ventricular dimension between cardiac α-actin A331P mutant transgenic mice and their wild-type littermates (Table I in the online-only Data Supplement). Although it is not known at present why the expression of cardiac α-actin A331P mutant did not induce hypertrophic cardiomyopathy, these results suggest that cardiac dysfunction of mActin-Tg mice is due to cardiac expression of the cardiac α-actin R312H mutant in the heart, not to high-level expression of the cardiac α-actin protein with the tag (lines 307 and 311).

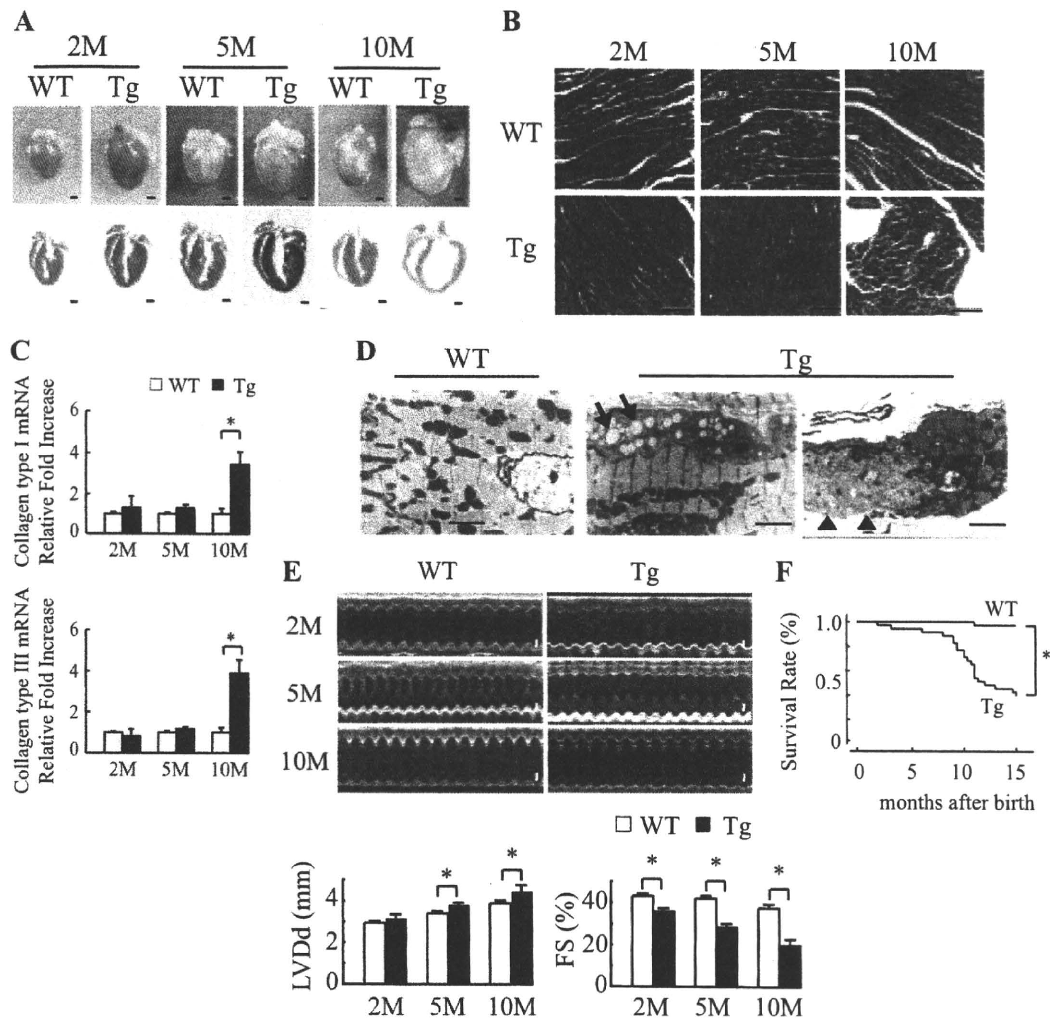

Figure 1. Mutated cardiac α-actin R312H transgenic mice. A, Gross morphology (top) and sections (bottom) of wild-type littermates (WT) or mActin-Tg (Tg) hearts at 2, 5, and 10 months (M) of age. Scale bar=1 mm. B, Masson trichrome staining. Scale bar=100 μm. C, Relative levels of collagen types I and III in hearts were normalized to GAPDH expression. *$P<0.05$ vs WT mice. n=4 in each group. D, Electron microscopic analyses. Cytoplasmic vacuolization (arrow) and lysis of myofibrils (arrowhead) were detected in the hearts of Tg mice. Scale bar=10 μm. E, Echocardiographic analysis. Scale bar=1 mm. LVDd indicates left ventricular end-diastolic dimension; FS, fractional shortening. *$P<0.05$. F, Kaplan-Meier survival curve. *$P<0.05$ vs WT mice. WT, n=32; Tg, n=37.

We used line 307, which expressed the cardiac α-actin R312H mutant at the highest levels, for further studies. The hearts in mActin-Tg mice were larger than those of wild-type littermates (Figure 1A), and heart weight and the ratio of heart weight to body weight were much increased in mActin-Tg mice (Table II in the online-only Data Supplement). Marked cardiac fibrosis was observed in mActin-Tg mice at 10 months of age, with increased expression of collagen types I and III (Figure 1B and 1C). Electron microscopic analyses showed that there were degenerated cardiomyocytes with an increase in vacuolar formation and lysis of myofibrils in mActin-Tg mice (Figure 1D). Echocardiography revealed that left ventricular dimension was gradually increased and that fractional shortening was reduced in mActin-Tg mice compared with wild-type littermates (Table II in the online-only Data Supplement and Figure 1E). The expression levels of ANP and SERCA2a were gradually increased and decreased in mActin-Tg mice, respectively (Figure III in the online-only Data Supplement). There was no significant difference in blood pressure, but heart rate was increased in mActin-Tg mice (Table II in the online-only Data Supplement), suggesting that the sympathetic nervous system is activated. Surface ECG monitoring showed low amplitude of the R wave in mActin-Tg mice (Table II in the online-only Data Supplement), which is often observed in human DCM patients. Many mActin-Tg mice died by 35 weeks of age (Figure 1F). Although telemetric ECG recording did not show life-threatening arrhythmia in mActin-Tg mice (data not shown), spontaneous Ca^{2+} sparks and Ca^{2+} waves were significantly increased in the cardiomyocytes of mActin-Tg mice (Table III in the online-only Data Supplement), suggesting that not only cardiac pump failure but also arrhythmia could be the cause of death. These phenotypes of mActin-Tg mice were quite similar to those of human DCM.

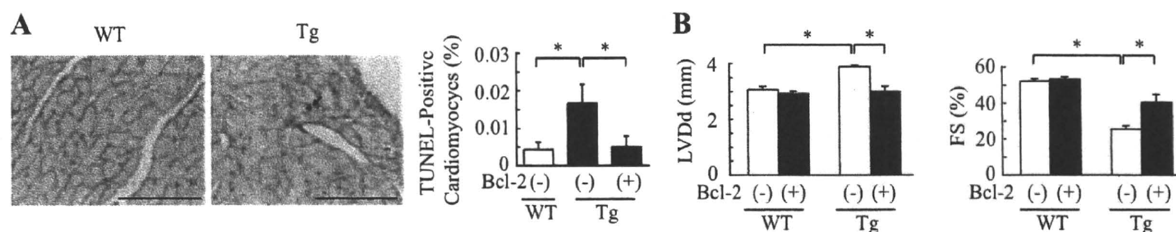

Figure 2. Increase in Bcl-2 preserves cardiac function in mActin-Tg mice. A, Double immunostaining for TUNEL (black) and dystrophin (red) of the heart (left). The graph indicates quantitative analyses of TUNEL-positive cardiomyocytes. Scale bar=100 μm. n=4 in each group. *$P<0.05$. B, Echocardiographic analyses at 5 months of age. *$P<0.05$. WT/Bcl-2(−), n=5; WT/Bcl-2(+), n=10; Tg/Bcl-2(−), n=10; Tg/Bcl-2(+), n=5. WT indicates wild-type littermates; Tg, mActin-Tg mice; LVDd, left ventricular end-diastolic dimension; and FS, fractional shortening.

Apoptotic Cardiomyocytes Are Increased in mActin-Tg Hearts

It has been reported that apoptosis of cardiomyocytes is observed in hearts of human DCM[10] and that cardiomyocyte death might cause cardiac dysfunction.[20] We thus examined apoptosis of cardiomyocytes by TUNEL labeling in left ventricular sections of wild-type littermates and mActin-Tg mice at 5 months of age. The number of TUNEL/dystrophin double-positive cardiomyocytes was significantly larger in mActin-Tg mice compared with wild-type littermates (Figure 2A). To examine whether the increase in apoptotic cardiomyocytes causes cardiac dysfunction in mActin-Tg mice, we generated double-transgenic mice by crossing mActin-Tg mice and the transgenic mice, which overexpress the antiapoptotic protein Bcl-2 in cardiomyocytes [mActin(+)/Bcl-2(+)-DTg].[14] The number of apoptotic cardiomyocytes in mActin(+)/Bcl-2(+)-DTg mice was significantly less compared with mActin-Tg mice (Figure 2A). Echocardiography revealed that the left ventricular dimension was smaller and fractional shortening was better in mActin(+)/Bcl-2(+)-DTg mice than in mActin-Tg mice at 5 months of age (Figure 2B), suggesting that the increase in apoptotic cardiomyocytes causes cardiac dysfunction in the DCM mouse model.

p53 Is Involved in Cardiomyocyte Apoptosis in mActin-Tg Mice

To clarify the mechanisms of how the cardiac α-actin R312H mutant induces apoptosis of cardiomyocytes, we examined expression levels of apoptosis-related proteins by Western blot analyses. The protein levels of p53 and Bax were higher in mActin-Tg mice compared with wild-type littermates (Figure 3A). Several key proapoptotic genes have been reported to be positively regulated by p53,[21] and increased expression of p53 induces left ventricular dilatation and dysfunction in several types of mice.[22,23] To determine the role of p53 in gene mutation–induced DCM, we crossed mActin-Tg mice and heterozygous p53-deficient mice [p53(+/−)]. Because many of homozygous p53-deficient mice [p53(−/−)] died of tumors before 5 months of age,[17] we used heterozygous p53-deficient mice [p53(+/−)] for this study. Echocardiography revealed that left ventricular dimension was smaller and fractional shortening was better in mActin-Tg/p53(+/−) mice than in mActin-Tg/p53(+/+) mice at 5 months of age (Figure 3B). Loss of a single p53 allele attenuated the increase of Bax (Figure 3C) and reduced the number of apoptotic cardiomyocytes in mActin-Tg mice (Figure 3D). These results suggest that p53-induced cardiomyocyte apoptosis induces dilatation and dysfunction of the left ventricle in the DCM mouse model.

Myofilament Calcium Sensitivity Is Decreased and Calcium-Dependent Enzymes Are Activated in mActin-Tg Mice

Many gene mutations associated with DCM have been reported to induce the decrease of myofilament Ca^{2+} sensi-

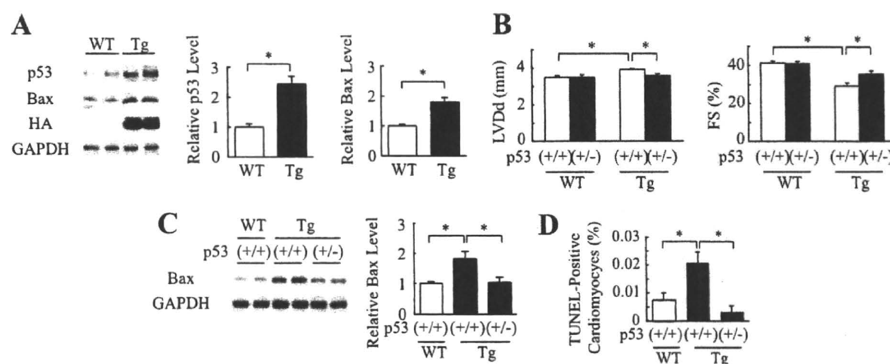

Figure 3. Inhibition of p53 preserves cardiac function in mActin-Tg mice. A, Western blot analyses in the hearts of wild-type littermates (WT) or mActin-Tg (Tg) mice at 5 months of age. The graph indicates relative protein levels of p53 (n=8 in each group) or Bax (n=10 in each group). *$P<0.05$. B, Echocardiographic analyses at 5 months of age. WT/p53(+/+), n=12; WT/p53(+/−), n=10; Tg/p53(+/+), n=19; Tg/p53(+/−), n=14. *$P<0.05$. C, Western blot analyses in the hearts. The graph indicates relative protein levels of Bax. n=6 in each group. *$P<0.05$. D, Quantitative analyses of TUNEL-positive cardiomyocytes. n=5 in each group. *$P<0.05$.

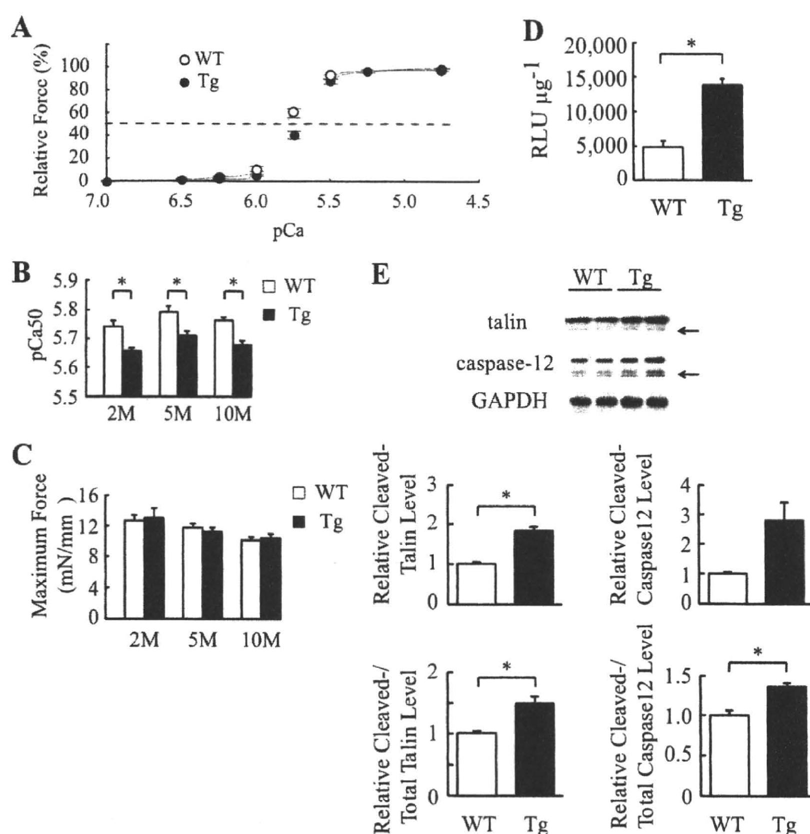

Figure 4. Myofilament Ca^{2+} sensitivity is decreased and Ca^{2+}-dependent enzymes are activated in mActin-Tg mice (Tg). A, Force-pCa relationship in skinned cardiac muscle fiber at 5 months of age. The broken line indicates pCa50. Wild-type (WT; n=11) and Tg (n=10) fibers were prepared from 3 isolated hearts. B, Ca^{2+} sensitivity (pCa50) of force-pCa relationships in skinned cardiac muscle fibers at 2, 5, and 10 months (M) of age. *$P<0.05$. C, Maximum force-generating capabilities. Fibers (n=9 to 11) were prepared from 3 isolated hearts of each group. D, The NFAT–luciferase reporter activity (RLU μg^{-1}) in the hearts at 5 months of age. n=4 in each group. *$P<0.05$. E, Western blot analyses in the hearts. Arrows indicate the calpain cleaved forms of talin and caspase-12. The graph indicates relative protein levels of cleaved talin or caspase-12 and ratio of cleaved forms to total proteins. n=4 in each group. *$P<0.05$.

tivity.[7] We examined myofilament Ca^{2+} sensitivity in mActin-Tg mice. The force-pCa relationship was shifted rightward in mActin-Tg mice compared with wild-type littermates (Figure 4A). The pCa value at half-maximal force generation (pCa50, an index of Ca^{2+} sensitivity) was significantly lower in mActin-Tg mice (Figure 4B), suggesting that skinned cardiac muscle fibers prepared from mActin-Tg mice show a decrease in Ca^{2+} sensitivity of force generation. The degree was the same between 2 and 10 months of age (Figure 4B), suggesting that the reduction in Ca^{2+} sensitivity is not a result of cardiac dysfunction. Despite the reduced Ca^{2+} sensitivity, there was no significant difference in maximum force-generating capabilities between wild-type littermates and mActin-Tg mice (Figure 4C). The decrease in myofilament Ca^{2+} sensitivity is expected to influence intracellular Ca^{2+} handling in cardiomyocytes of mActin-Tg mice. To clarify whether intracellular Ca^{2+} levels in cardiomyocytes are changed in mActin-Tg mice, we examined the activity of Ca^{2+}-dependent enzymes such as calcineurin and calpain. We generated double-transgenic mice by crossing mActin-Tg mice and the transgenic mice carrying a luciferase reporter driven by a cluster of NFAT binding sites, which is activated by calcineurin-dependent NFAT proteins.[15] The NFAT–luciferase reporter activity was higher in mActin-Tg mice than in wild-type littermates at 5 months of age (Table IV in the online-only Data Supplement and Figure 4D). Furthermore, the ratio of the calpain-induced cleaved forms of talin and caspase-12 to total proteins was significantly increased in mActin-Tg mice compared with wild-type littermates (Figure 4E). We next examined Ca^{2+} transients in cardiomyocytes using fluo-3AM (Figure IVA in the online-only Data Supplement). Although the time to peak amplitude of Ca^{2+} was significantly slower in mActin-Tg mice than in wild-type littermates (Figure IVB in the online-only Data Supplement), there was no significant difference in peak amplitude between wild-type littermates and mActin-Tg mice at 2 and 10 months of age (Figure IVC in the online-only Data Supplement). The expression levels of SERCA2a, but not Na^+/Ca^{2+} exchanger, were decreased in mActin-Tg mice (Figure III in the online-only Data Supplement).

CaMKIIδ Is Activated in mActin-Tg Mice

It has been reported that among Ca^{2+}-dependent proteins, expression of CaMKIIδ is increased in human DCM hearts[24] and that overexpression of CaMKIIδ induces heart failure in mice.[25,26] We thus examined the expression and phosphorylation of CaMKIIδ and phosphorylation of its target protein, phospholamban (Thr17). The protein levels of total (both CaMKIIδB and CaMKIIδC) and phosphorylated CaMKIIδ and of phosphorylated phospholamban (Thr17) were increased in mActin-Tg mice compared with wild-type littermates (Figure 5A and Figure VA in the online-only Data Supplement), suggesting that CaMKIIδ is activated in mActin-Tg mice. The protein levels of phosphorylated phospholamban (Ser16), which is activated by protein kinase A, were also increased in mActin-Tg mice (Figure 5A).

Because it has been reported that the sympathetic nervous system is activated in failing hearts and that β-adrenergic

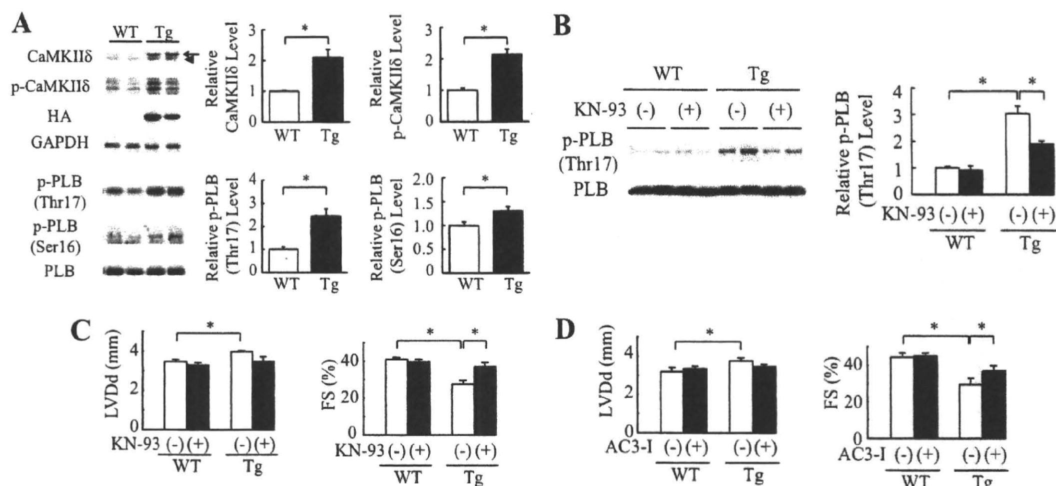

Figure 5. CaMKIIδ is activated in mActin-Tg mice. A, Western blot analyses in the hearts of wild-type littermates (WT) or mActin-Tg (Tg) mice at 5 months of age. The graph indicates relative protein levels of total and phosphorylated CaMKIIδ (p- CaMKIIδ) or phosphorylated phospholamban (p-PLB). Arrow and arrowhead indicate CaMKIIδB and CaMKIIδC, respectively. n=6 in each group. *$P<0.05$. B, Western blot analyses in the hearts at 5 months of age. The graph indicates relative protein levels of p-PLB (Thr17). n=4 in each group. *$P<0.05$. C and D, Echocardiographic analyses at 5 months of age. WT/KN-93(−), n=11; WT/KN-93(+), n=7; Tg/KN-93(−), n=8; Tg/KN-93(+), n=6; WT/AC3-I(−), n=8; WT/AC3-I(+), n=18; Tg/AC3-I(−), n=10; Tg/AC3-I(+), n=14. KN indicates KN-93; LVDd, left ventricular end-diastolic dimension; and FS, fractional shortening. *$P<0.05$.

receptor signal activates CaMKIIδ,[27] we treated mActin-Tg mice with the β-blocker bisoprolol to clarify the relationship between β-adrenergic receptor signal and activation of CaMKIIδ. The treatment with bisoprolol ameliorated cardiac dysfunction of mActin-Tg mice, and there was no significant difference in cardiac function between wild-type littermates and mActin Tg mice with bisoprolol treatment (Figure VB in the online-only Data Supplement). Furthermore, the increase in CaMKIIδ levels in mActin-Tg mice was prevented by bisoprolol treatment (Figure VC in the online-only Data Supplement), suggesting that the activation of CaMKIIδ in mActin-Tg mice might be due to activation of β-adrenergic receptor signaling.

To test whether activation of CaMKIIδ induces cardiac dysfunction, we first treated mActin-Tg mice with KN-93, a CaMKII inhibitor. Levels of both phosphorylated phospholamban (Thr17) and phospholamban (Ser16) were decreased by KN-93 treatment in mActin-Tg mice (Figure 5B and Figure VD in the online-only Data Supplement). Echocardiography revealed that KN-93 treatment prevented left ventricular dilatation and preserved cardiac function in mActin-Tg mice (Figure 5C). On the other hand, KN-92, an inactive derivative of KN-93, did not show any effects (Figure VE in the online-only Data Supplement). To confirm the role of CaMKIIδ in mActin-Tg mice, we crossed mActin-Tg mice and AC3-I mice, which expressed the CaMKII-inhibitory peptide AC3-I in the heart [mActin(+)/AC3-I(+)-DTg].[16] Echocardiography revealed that fractional shortening was better in mActin(+)/AC3-I(+)-DTg mice than in mActin(+)/AC3-I(−)-Tg mice (Figure 5D), suggesting that the activation of CaMKIIδ in the DCM mouse model induces left ventricular dilatation and contractile dysfunction.

We next examined the relation between CaMKIIδ activation and p53. The increase in p53 was attenuated by treatment with KN-93 or overexpression of AC3-I (Figure 6A and Figure VIA in the online-only Data Supplement). Furthermore, KN-93 treatment inhibited the increase in Bax expression and TUNEL-positive cardiomyocytes (Figure 6A and 6B). It has been reported that CaMKIIδC, but not CaMKIIδB, induces cardiomyocyte death.[27–29] To clarify the mechanism of how CaMKIIδ increases protein levels of p53 and which

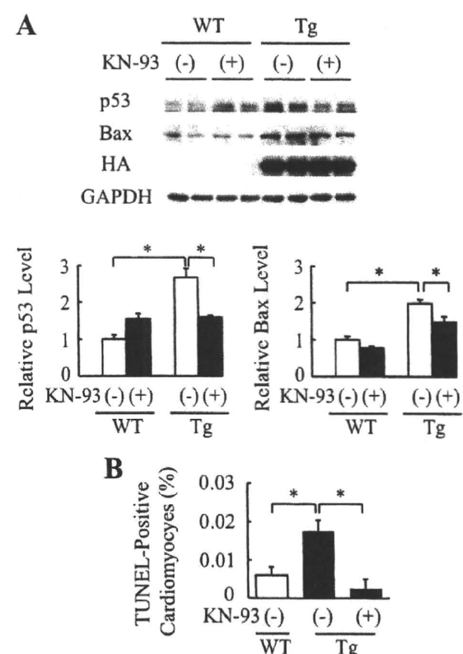

Figure 6. CaMKIIδ regulates expression of p53 in cardiomyocytes. A, Western blot analyses in the hearts of wild-type littermates (WT) or mActin-Tg (Tg) mice. The graph indicates relative protein levels of p53 or Bax. n=4 in each group. *$P<0.05$. B, Quantitative analyses of TUNEL-positive cardiomyocytes. n=5 in each group. *$P<0.05$.

CaMKIIδ, δB or δC, plays an important role in apoptosis of cardiomyocytes, we transfected constitutively active forms of CaMKIIδ (caCaMKIIδ) into cardiomyocytes. Only caCaMKIIδC, not caCaMKIIδB, increased protein levels of p53 (Figure VIB in the online-only Data Supplement). Furthermore, p53 protein levels in caCaMKIIδC-transfected cardiomyocytes did not increase with MG132 treatment compared with MOCK-treated cardiomyocytes (Figure VIC in the online-only Data Supplement). These results suggest that activation of CaMKIIδC increases apoptotic cardiomyocytes at least in part via stabilization of p53 in the DCM mouse model.

Discussion

In the present study, we established a novel mouse model of DCM to clarify the mechanisms of how mutant genes lead to DCM (Table II in the online-only Data Supplement and Figure 1). The mice expressing cardiac α-actin R312H mutant in the heart, which has been reported to cause DCM in humans,[5] showed dilatation and dysfunction of left ventricle with an increase in ANP messenger RNA levels, which is consistent with human heart failure (Figure 1A and 1E and Table II and Figure III in the online-only Data Supplement). Higher heart rate and hyperphosphorylated phospholamban (Ser16) (Table II in the online-only Data Supplement and Figure 5A) suggest the activation of the sympathetic nervous system to compensate for reduced cardiac systolic function, resulting in an increase in spontaneous Ca^{2+} sparks and Ca^{2+} waves (Table III in the online-only Data Supplement). Myofilament Ca^{2+} sensitivity was decreased in mActin-Tg mice even at 2 months of age (Figure 4B), when cardiac phenotypes such as left ventricular dilatation and cardiac fibrosis were not recognized (Table II in the online-only Data Supplement and Figure 1). These results suggest that the decrease in myofilament Ca^{2+} sensitivity is a primary cause of, not a secondary result from, cardiac dysfunction. Because these phenotypes were quite similar to those of human DCM, mActin-Tg mice are useful for examining the underlying mechanisms of how gene mutations lead to DCM.

There was no significant difference in the peak amplitude of Ca^{2+} transients between wild-type littermates and mActin-Tg mice (Figure IVC in the online-only Data Supplement), suggesting that global Ca^{2+} levels underlying each contractile cycle do not differ between the 2 groups. It has been reported that the peak amplitude of Ca^{2+} transients, which is associated with decreased Ca^{2+} sensitivity and systolic dysfunction, is higher in another mouse model of DCM, [7] suggesting that Ca^{2+} transients are augmented to compensate for decreased myofilament Ca^{2+} sensitivity in this model. In mActin-Tg mice, despite the preserved Ca^{2+} transients (Figure IVC in the online-only Data Supplement), global cardiac function was gradually impaired (Table II in the online-only Data Supplement). Local Ca^{2+} concentration has been reported to be important for the activation of Ca^{2+}-dependent enzymes such as calcineurin, calpain, and CaMKII in cardiomyocytes.[30] The activation of these molecules in mActin-Tg mice (Figures 4D, 4E, and 5A) might be attributed to an increase in local Ca^{2+} levels. It still remains to be determined whether local Ca^{2+} levels are really increased and, if so, how the decrease in Ca^{2+} sensitivity increases local Ca^{2+} levels.

Recent reports have shown that CaMKIIδ plays a crucial role in cardiovascular diseases.[16,31] The transgenic mice that overexpressed CaMKIIδ showed heart failure with systolic dysfunction and left ventricular dilatation.[25,26] In this study, CaMKIIδ was activated in the hearts of mActin-Tg mice (Figure 5A), and inhibition of CaMKIIδ by KN-93 or AC3-I ameliorated cardiac dysfunction in mActin-Tg mice (Figure 5C and 5D), suggesting that CaMKIIδ also plays an important role in gene mutation–induced cardiac dysfunction.

It has been reported that apoptosis of cardiomyocytes is observed in hearts of human DCM[10] and that cardiomyocyte death could cause cardiac dysfunction.[20] However, it remains unclear whether apoptosis of cardiomyocytes causes cardiac dysfunction and how cardiomyocyte apoptosis is induced in hearts of DCM. In this study, there were more apoptotic cardiomyocytes in mActin-Tg mice (Figure 2A), and cardiac function was improved by protecting cardiomyocytes from apoptosis through overexpression of Bcl-2 (Figure 2B). These results suggest that cardiomyocyte apoptosis plays a crucial role in the development of DCM. Several key proapoptotic and antiapoptotic genes have been reported to be positively or negatively regulated by p53, and increased expression of p53 induces left ventricular dilatation and dysfunction in mice deficient in MDM4, an E3 ligase for p53.[23] Furthermore, we have recently demonstrated that p53 is critically involved in pressure overload–induced cardiac dysfunction.[22] The protein levels of p53 were increased in mActin-Tg mice (Figure 3A), and loss of a single p53 allele reduced the number of apoptotic cardiomyocytes (Figure 3D) and improved cardiac function (Figure 3B). These results suggest that p53 is critically involved in induction of cardiomyocyte apoptosis, resulting in left ventricular dysfunction in the mouse model of DCM.

The present study indicates that p53 might be a therapeutic target for DCM. In this study, CaMKIIδ was activated in the hearts of mActin-Tg mice (Figure 5A), and the inhibition of CaMKIIδ attenuated the increase in p53 protein levels (Figure 6A and Figure VIA in the online-only Data Supplement), suggesting that CaMKIIδ regulates protein levels of p53 in the DCM model mice. Although it remains to be determined how CaMKIIδ regulates protein levels of p53, inhibition of CaMKIIδ may become a new therapeutic strategy for DCM patients by reducing p53 protein levels in the heart.

Limitations

This study has a couple limitations. First, we cannot completely rule out the nonspecific effects of overexpression of cardiac α-actin gene with tag because of a lack of transgenic mice that overexpress wild-type cardiac α-actin gene. However, we think the cardiac dysfunction observed in mActin-Tg was due to cardiac expressions of the cardiac α-actin R312H mutant in the heart, not to high-level expressions of the cardiac α-actin protein with tag because of the following reasons: We obtained 3 independent founders of the transgenic mice, and the reduction in cardiac function was well correlated with protein levels of the cardiac α-actin R312H mutant (Figure I in the online-only Data Supplement). An-

other transgenic mouse that expressed cardiac α-actin A331P mutant with an HA tag in the heart did not show cardiac dysfunction (Table I in the online-only Data Supplement), although the protein levels of the mutant in the A331P mutant transgenic mice were almost same as those of the R312H mutant in line 307, which had the highest expression (Figure II in the online-only Data Supplement). Second, we found that CaMKIIδC increases p53 protein levels mainly by its stabilization, but the underlying mechanisms remain to be determined.

Acknowledgments

We thank J. Robbins (Children's Hospital Research Foundation, Cincinnati, Ohio) for a fragment of α-myosin heavy chain gene promoter, J.D. Molkentin (Children's Hospital Research Foundation, Cincinnati, Ohio) for NFAT–luciferase reporter transgenic mice, M.D. Schneider (Imperial College, London, UK) for Bcl-2 transgenic mice, and E.N. Olson (UT Southwestern Medical Center, Dallas, Tex) for constitutively active forms of CaMKIIδ. We thank E. Fujita, R. Kobayashi, Y. Ishiyama, M. Ikeda, I. Sakamoto, A. Furuyama, and Y. Ohtsuki for technical support, as well as M. Iiyama, K. Matsumoto, Y. Ishikawa, and Y. Yasukawa for animal care.

Sources of Funding

This work was supported by a Grant-in-Aid for Scientific Research on Priority Areas (to Dr Komuro) and a Grant-in-Aid for Scientific Research (C) (20590857 to Dr Oka) from the Ministry of Education, Culture, Sports, Science and Technology; the Japan Heart Foundation/Novartis Grant for Research Award on Molecular and Cellular Cardiology; Japan Foundation for Applied Enzymology; Suzuken Memorial Foundation; and Mitsubishi Pharma Research Foundation (to Dr Toko). This work was supported by National Institutes of Health grants R01 HL079031, R01 HL070250, and R01 HL096652 and by the Fondation Leducq Award to the Alliance for Calmodulin Kinase Signaling in Heart Disease (to Dr Anderson).

Disclosures

Dr Anderson is named on patents claiming to treat heart failure by CaMKII inhibition and is a cofounder of Allosteros. The other authors report no conflicts.

References

1. Michels VV, Moll PP, Miller FA, Tajik AJ, Chu JS, Driscoll DJ, Burnett JC, Rodeheffer RJ, Chesebro JH, Tazelaar HD. The frequency of familial dilated cardiomyopathy in a series of patients with idiopathic dilated cardiomyopathy. *N Engl J Med*. 1992;326:77–82.
2. Maron BJ, Towbin JA, Thiene G, Antzelevitch C, Corrado D, Arnett D, Moss AJ, Seidman CE, Young JB. Contemporary definitions and classification of the cardiomyopathies: an American Heart Association scientific statement from the Council on Clinical Cardiology, Heart Failure and Transplantation Committee; Quality of Care and Outcomes Research and Functional Genomics and Translational Biology Interdisciplinary Working Groups; and Council on Epidemiology and Prevention. *Circulation*. 2006;113:1807–1816.
3. Ahmad F, Seidman JG, Seidman CE. The genetic basis for cardiac remodeling. *Annu Rev Genomics Hum Genet*. 2005;6:185–216.
4. Knoll R, Hoshijima M, Hoffman HM, Person V, Lorenzen-Schmidt I, Bang ML, Hayashi T, Shiga N, Yasukawa H, Schaper W, McKenna W, Yokoyama M, Schork NJ, Omens JH, McCulloch AD, Kimura A, Gregorio CC, Poller W, Schaper J, Schultheiss HP, Chien KR. The cardiac mechanical stretch sensor machinery involves a Z disc complex that is defective in a subset of human dilated cardiomyopathy. *Cell*. 2002;111:943–955.
5. Olson TM, Michels VV, Thibodeau SN, Tai YS, Keating MT. Actin mutations in dilated cardiomyopathy, a heritable form of heart failure. *Science*. 1998;280:750–752.
6. Towbin JA, Bowles NE. Genetic abnormalities responsible for dilated cardiomyopathy. *Curr Cardiol Rep*. 2000;2:475–480.
7. Du CK, Morimoto S, Nishii K, Minakami R, Ohta M, Tadano N, Lu QW, Wang YY, Zhan DY, Mochizuki M, Kita S, Miwa Y, Takahashi-Yanaga F, Iwamoto T, Ohtsuki I, Sasaguri T. Knock-in mouse model of dilated cardiomyopathy caused by troponin mutation. *Circ Res*. 2007;101:185–194.
8. Kawada T, Masui F, Tezuka A, Ebisawa T, Kumagai H, Nakazawa M, Toyo-Oka T. A novel scheme of dystrophin disruption for the progression of advanced heart failure. *Biochim Biophys Acta*. 2005;1751:73–81.
9. Kyoi S, Otani H, Matsuhisa S, Akita Y, Tatsumi K, Enoki C, Fujiwara H, Imamura H, Kamihata H, Iwasaka T. Opposing effect of p38 MAP kinase and JNK inhibitors on the development of heart failure in the cardiomyopathic hamster. *Cardiovasc Res*. 2006;69:888–898.
10. Olivetti G, Abbi R, Quaini F, Kajstura J, Cheng W, Nitahara JA, Quaini E, Di Loreto C, Beltrami CA, Krajewski S, Reed JC, Anversa P. Apoptosis in the failing human heart. *N Engl J Med*. 1997;336:1131–1141.
11. Bulfield G, Siller WG, Wight PA, Moore KJ. X chromosome-linked muscular dystrophy (mdx) in the mouse. *Proc Natl Acad Sci U S A*. 1984;81:1189–1192.
12. Cooper BJ, Winand NJ, Stedman H, Valentine BA, Hoffman EP, Kunkel LM, Scott MO, Fischbeck KH, Kornegay JN, Avery RJ, Williams JR, Schmickel RD, Sylvester JE. The homologue of the Duchenne locus is defective in X-linked muscular dystrophy of dogs. *Nature*. 1988;334:154–156.
13. Nigro V, Okazaki Y, Belsito A, Piluso G, Matsuda Y, Politano L, Nigro G, Ventura C, Abbondanza C, Molinari AM, Acampora D, Nishimura M, Hayashizaki Y, Puca GA. Identification of the Syrian hamster cardiomyopathy gene. *Hum Mol Genet*. 1997;6:601–607.
14. Tanaka M, Nakae S, Terry RD, Mokhtari GK, Gunawan F, Balsam LB, Kaneda H, Kofidis T, Tsao PS, Robbins RC. Cardiomyocyte-specific Bcl-2 overexpression attenuates ischemia-reperfusion injury, immune response during acute rejection, and graft coronary artery disease. *Blood*. 2004;104:3789–3796.
15. Wilkins BJ, Dai YS, Bueno OF, Parsons SA, Xu J, Plank DM, Jones F, Kimball TR, Molkentin JD. Calcineurin/NFAT coupling participates in pathological, but not physiological, cardiac hypertrophy. *Circ Res*. 2004;94:110–118.
16. Zhang R, Khoo MS, Wu Y, Yang Y, Grueter CE, Ni G, Price EE Jr, Thiel W, Guatimosim S, Song LS, Madu EC, Shah AN, Vishnivetskaya TA, Atkinson JB, Gurevich VV, Salama G, Lederer WJ, Colbran RJ, Anderson ME. Calmodulin kinase II inhibition protects against structural heart disease. *Nat Med*. 2005;11:409–417.
17. Donehower LA, Harvey M, Slagle BL, McArthur MJ, Montgomery CA Jr, Butel JS, Bradley A. Mice deficient for p53 are developmentally normal but susceptible to spontaneous tumours. *Nature*. 1992;356:215–221.
18. VanGuilder HD, Vrana KE, Freeman WM. Twenty-five years of quantitative PCR for gene expression analysis. *Biotechniques*. 2008;44:619–626.
19. Olson TM, Doan TP, Kishimoto NY, Whitby FG, Ackerman MJ, Fananapazir L. Inherited and de novo mutations in the cardiac actin gene cause hypertrophic cardiomyopathy. *J Mol Cell Cardiol*. 2000;32:1687–1694.
20. Wencker D, Chandra M, Nguyen K, Miao W, Garantziotis S, Factor SM, Shirani J, Armstrong RC, Kitsis RN. A mechanistic role for cardiac myocyte apoptosis in heart failure. *J Clin Invest*. 2003;111:1497–1504.
21. Ryan KM, Phillips AC, Vousden KH. Regulation and function of the p53 tumor suppressor protein. *Curr Opin Cell Biol*. 2001;13:332–337.
22. Sano M, Minamino T, Toko H, Miyauchi H, Orimo M, Qin Y, Akazawa H, Tateno K, Kayama Y, Harada M, Shimizu I, Asahara T, Hamada H, Tomita S, Molkentin JD, Zou Y, Komuro I. p53-induced inhibition of Hif-1 causes cardiac dysfunction during pressure overload. *Nature*. 2007;446:444–448.
23. Xiong S, Van Pelt CS, Elizondo-Fraire AC, Fernandez-Garcia B, Lozano G. Loss of Mdm4 results in p53-dependent dilated cardiomyopathy. *Circulation*. 2007;115:2925–2930.
24. Hoch B, Meyer R, Hetzer R, Krause EG, Karczewski P. Identification and expression of delta-isoforms of the multifunctional Ca2+/calmodulin-dependent protein kinase in failing and nonfailing human myocardium. *Circ Res*. 1999;84:713–721.
25. Zhang T, Johnson EN, Gu Y, Morissette MR, Sah VP, Gigena MS, Belke DD, Dillmann WH, Rogers TB, Schulman H, Ross J Jr, Brown JH. The cardiac-specific nuclear delta(B) isoform of Ca2+/calmodulin-dependent protein kinase II induces hypertrophy and dilated cardiomyopathy associated with increased protein phosphatase 2A activity. *J Biol Chem*. 2002;277:1261–1267.

26. Zhang T, Maier LS, Dalton ND, Miyamoto S, Ross J Jr, Bers DM, Brown JH. The deltaC isoform of CaMKII is activated in cardiac hypertrophy and induces dilated cardiomyopathy and heart failure. *Circ Res*. 2003;92: 912–919.
27. Zhu WZ, Wang SQ, Chakir K, Yang D, Zhang T, Brown JH, Devic E, Kobilka BK, Cheng H, Xiao RP. Linkage of beta1-adrenergic stimulation to apoptotic heart cell death through protein kinase A-independent activation of Ca2+/calmodulin kinase II. *J Clin Invest*. 2003;111:617–625.
28. Peng W, Zhang Y, Zheng M, Cheng H, Zhu W, Cao CM, Xiao RP Cardioprotection by CaMKII-deltaB is mediated by phosphorylation of heat shock factor 1 and subsequent expression of inducible heat shock protein 70. *Circ Res*. 2010;106:102–110.
29. Zhu W, Woo AY, Yang D, Cheng H, Crow MT, Xiao RP. Activation of CaMKIIdeltaC is a common intermediate of diverse death stimuli-induced heart muscle cell apoptosis. *J Biol Chem*. 2007;282: 10833–10839.
30. Wu X, Zhang T, Bossuyt J, Li X, McKinsey TA, Dedman JR, Olson EN, Chen J, Brown JH, Bers DM. Local InsP3-dependent perinuclear Ca2+ signaling in cardiac myocyte excitation-transcription coupling. *J Clin Invest*. 2006;116:675–682.
31. Ling H, Zhang T, Pereira L, Means CK, Cheng H, Gu Y, Dalton ND, Peterson KL, Chen J, Bers D, Heller Brown J. Requirement for Ca2+/calmodulin-dependent kinase II in the transition from pressure overload-induced cardiac hypertrophy to heart failure in mice. *J Clin Invest*. 2009;119:1230–1240.

CLINICAL PERSPECTIVE

Heart failure is an important cause of morbidity and mortality in many industrial countries, and dilated cardiomyopathy (DCM) is one of its major causes. Molecular genetic studies over the last 2 decades have revealed many mutations of various genes in DCM patients, but the precise mechanisms of how such mutations lead to DCM remain largely unknown partly because of a lack of good animal models of DCM. Here, we established the mouse model of DCM by expressing a mutated cardiac α-actin gene, which has been reported in patients with DCM, in the heart. The transgenic mice showed gradual dilatation and dysfunction of the left ventricle, resulting in death by heart failure. These phenotypes of the transgenic mice were quite similar to those of human DCM. The number of apoptotic cardiomyocytes and protein levels of p53 were increased in the hearts of the DCM mice. Overexpression of Bcl-2, an antiapoptotic factor, or downregulation of p53 decreased the number of apoptotic cardiomyocytes and improved cardiac function. The DCM mice showed activation of CaMKIIδ. The inhibition of CaMKIIδ prevented the increase in p53 and apoptotic cardiomyocytes and ameliorated cardiac function. These results suggest that CaMKIIδ plays a critical role in the development of heart failure in part by accumulation of p53 and induction of cardiomyocyte apoptosis in the DCM mouse model. The inhibition of CaMKIIδ may become a new therapeutic strategy for DCM patients.

Research article

Sonic hedgehog is a critical mediator of erythropoietin-induced cardiac protection in mice

Kazutaka Ueda,[1] Hiroyuki Takano,[1] Yuriko Niitsuma,[1,2] Hiroshi Hasegawa,[1] Raita Uchiyama,[1] Toru Oka,[1] Masaru Miyazaki,[2] Haruaki Nakaya,[3] and Issei Komuro[1]

[1]Department of Cardiovascular Science and Medicine, [2]Department of General Surgery, and [3]Department of Pharmacology, Chiba University Graduate School of Medicine, Chiba, Japan.

Erythropoietin reportedly has beneficial effects on the heart after myocardial infarction, but the underlying mechanisms of these effects are unknown. We here demonstrate that sonic hedgehog is a critical mediator of erythropoietin-induced cardioprotection in mice. Treatment of mice with erythropoietin inhibited left ventricular remodeling and improved cardiac function after myocardial infarction, independent of erythropoiesis and the mobilization of bone marrow–derived cells. Erythropoietin prevented cardiomyocyte apoptosis and increased the number of capillaries and mature vessels in infarcted hearts by upregulating the expression of angiogenic cytokines such as VEGF and angiopoietin-1 in cardiomyocytes. Erythropoietin also increased the expression of sonic hedgehog in cardiomyocytes, and inhibition of sonic hedgehog signaling suppressed the erythropoietin-induced increase in angiogenic cytokine expression. Furthermore, the beneficial effects of erythropoietin on infarcted hearts were abolished by cardiomyocyte-specific deletion of sonic hedgehog. These results suggest that erythropoietin protects the heart after myocardial infarction by inducing angiogenesis through sonic hedgehog signaling.

Introduction

Recent medical advances have improved survival rates of patients with acute myocardial infarction (MI), whereas the number of patients showing heart failure after MI has increased in recent years (1). LV remodeling, which includes dilatation of the ventricle and increased interstitial fibrosis, is the critical process that underlies the progression to heart failure (1). Although pharmacological therapies are effective, heart failure is still one of the leading causes of death worldwide (2). It is thus important to elucidate a novel approach to prevent LV remodeling after MI.

Several hematopoietic cytokines including erythropoietin (EPO), G-CSF, and stem cell factor have been reported to prevent cardiac remodeling and dysfunction after MI in various animal models (3–5). EPO, a major regulator of erythroid progenitors, has attracted great attention because its administration induced significant improvements in the clinical status and LV function of patients with congestive heart failure (6, 7). Although several mechanisms of cardioprotective effects by EPO have been suggested, the precise mechanisms remain largely unknown (8–14). Treatment with EPO reverses the decreased oxygen-carrying capacity associated with anemia, which is often observed in patients with heart failure (8). EPO has also been reported to mobilize endothelial progenitor cells (EPCs) from bone marrow, leading to neovascularization in the heart (9). In addition, since EPO receptors (EPORs) are expressed in various types of cells including cardiomyocytes, EPO may have direct protective effects on cardiomyocytes (10–14).

In the present study, we investigated the mechanisms of how EPO induced cardioprotection after MI. We observed that EPO directly prevented apoptotic death of cardiomyocytes and enhanced the expression of angiogenic cytokines, which induced robust angiogenesis, leading to the improvement of contractile function after MI. EPO also increased expression levels of sonic hedgehog (Shh) in cardiomyocytes, and the inhibition of Shh signaling abolished the EPO-induced increases of angiogenic cytokine production in cardiomyocytes. In hearts of cardiac-specific inducible Shh knockout (Shh-MerCre) mice, EPO treatment failed to upregulate angiogenic cytokines, enhance angiogenesis, and inhibit LV remodeling. Our results suggest that Shh is a key mediator of EPO-evoked cardioprotection in infarcted hearts.

Results

EPO prevents cardiac remodeling after MI. We subcutaneously administered EPO (10,000 U/kg/d) or saline immediately after coronary artery ligation until 4 days after MI. Fourteen days after MI, we histologically assessed the infarct size and examined cardiac function using echocardiography. Treatment with EPO significantly prevented enlargement of LV end-diastolic dimension (LVEDD) and reduction of fractional shortening (FS) and reduced the infarct size (fibrotic area/LV free wall) compared with saline treatment (Figure 1, A and B), suggesting that EPO prevents LV remodeling and dysfunction after MI.

The role of hematopoietic effects of EPO in cardioprotection (6, 7) was examined using transgene-rescued EPOR-null (RES) mice, which express EPORs only in the hematopoietic lineage (15). Although EPO treatment increased blood hemoglobin levels 7 days after MI in both WT and RES mice (Figure 2A), the cardioprotective effects of EPO were observed only in WT mice but not in the RES mice (Figure 1 and Figure 2B). EPO and saline did not show any significant differences in LVEDD, FS, or infarct size in the RES mice (Figure 2B), suggesting that erythropoiesis is not involved in the cardioprotective effects of EPO.

Authorship note: Kazutaka Ueda, Hiroyuki Takano, and Yuriko Niitsuma contributed equally to this work.

Conflict of interest: The authors have declared that no conflict of interest exists.

Citation for this article: *J Clin Invest.* 2010;120(6):2016–2029. doi:10.1172/JCI39896.

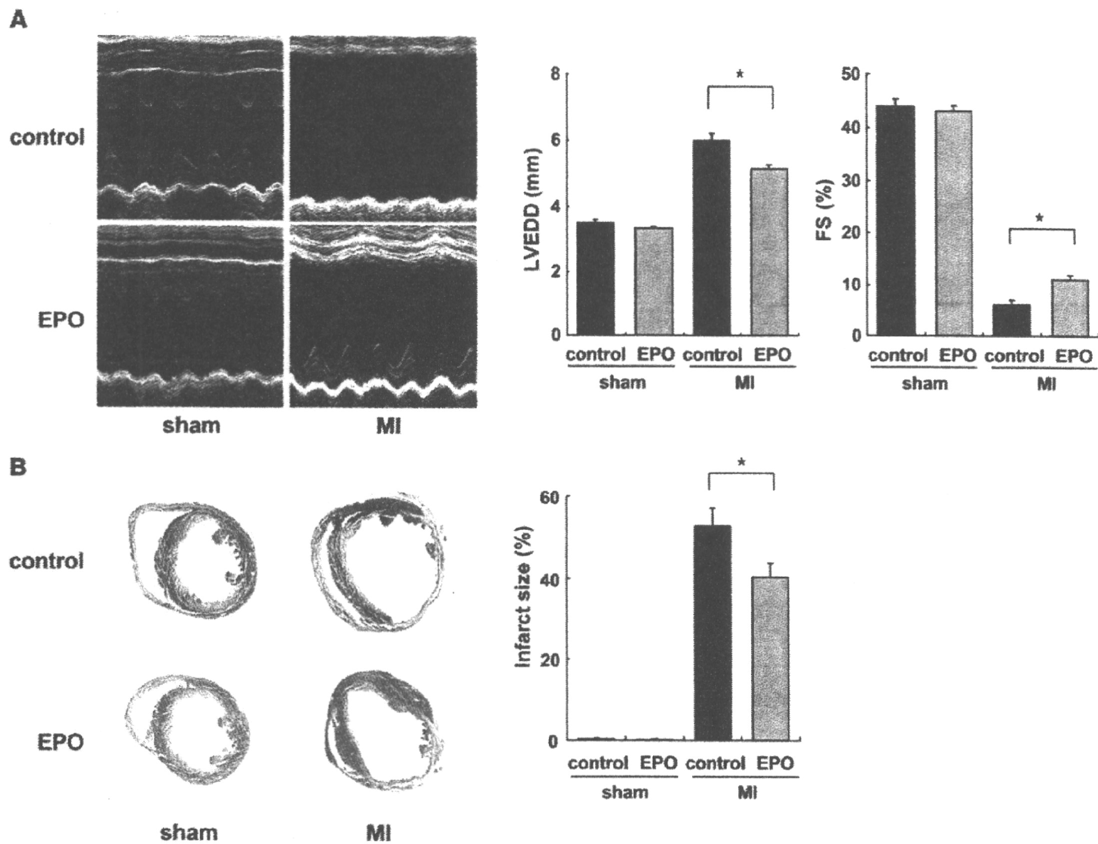

Figure 1
EPO prevents cardiac remodeling after MI. The effects of EPO treatment on LV function and infarct size were examined 14 days after operation. WT mice were subjected to MI or sham operation and treated with EPO or saline (control). (**A**) Echocardiographic analysis. (n = 8–10). (**B**) Masson trichrome staining of hearts and infarct size (n = 8–10). *$P < 0.01$.

To investigate whether EPO affects responses of inflammation and wound healing that may have an impact on LV remodeling after MI (16, 17), we examined macrophage infiltration and myofibroblast accumulation in the ischemic area after MI by immunohistochemical staining. The number of Mac3-positive macrophages was markedly decreased by EPO treatment 14 days after MI (Supplemental Figure 1A; supplemental material available with this article; doi:10.1172/JCI39896DS1). The number of α-SMA-positive myofibroblasts was significantly increased in EPO-treated hearts compared with saline-treated hearts (Supplemental Figure 1B).

We next determined whether EPO induced the mobilization of EPCs from bone marrow into peripheral blood using flow cytometry (9). After MI, EPO significantly increased the number of circulating CD34/Flk-1-double-positive EPCs in WT mice but not in the RES mice (Figure 2C). We produced MI in WT mice in which the bone marrow was replaced with cells derived from GFP-expressing mice. The hearts were excised 7 and 14 days after MI and immunohistochemically stained for PECAM. There were no differences in the number of GFP-positive cells and GFP/PECAM-double-positive cells in the border areas of EPO- and saline-treated infarcted hearts (Figure 2D), indicating that EPO did not enhance the homing of bone marrow-derived cells or increase the number of bone marrow-derived endothelial cells in the damaged hearts, although EPO induced mobilization of EPCs from bone marrow into peripheral circulation. In addition, EPO did not improve cardiac function or increase the number of vessels in infarcted hearts even in RES mice transplanted with bone marrow of WT mice (Figure 2E). It is thus unlikely that the EPO-mobilized bone marrow-derived cells contribute to the cardioprotective effects of EPO.

EPO inhibits cardiomyocyte apoptosis in infarcted hearts. Apoptotic death of cardiomyocytes has been suggested to cause LV remodeling and dysfunction (18). To determine the role of antiapoptotic effects of EPO in cardioprotection, we performed TUNEL staining of hearts 24 hours after MI. The number of TUNEL-positive cardiomyocytes in the border area was significantly smaller in EPO-treated mice than in saline-treated mice, while EPO treatment had no effect on cardiomyocyte apoptosis in RES mice (Figure 3A). Western blot analysis showed that EPO treatment markedly reduced the level of cleaved caspase-3 in hearts at 24 hours after MI (Figure 3B). TUNEL staining revealed that pretreatment with EPO significantly attenuated H_2O_2-induced apoptotic death in cultured cardiomyocytes of neonatal rats (Figure 3C). At 24 hours after exposing cardiomyocytes to H_2O_2, expression levels of the antiapoptotic protein Bcl-2 were decreased, whereas levels of cleaved caspase-3 were increased, and these changes were inhibited markedly by EPO pretreatment (Figure 3D). Annexin V staining

Figure 2

Erythroid hematogenesis is not required for the protective effects of EPO, and EPO does not accelerate the cardiac homing of bone marrow–derived cells after MI. WT and RES mice were subjected to MI and treated with EPO or saline (control). (**A**) Blood hemoglobin (Hb) levels 7 days after MI (n = 4). *P < 0.01. (**B**) Echocardiography and Masson trichrome staining were performed to analyze LV function and infarct size (n = 10). (**C**) Following MI and EPO treatment, the number of circulating CD34/Flk-1–double-positive EPCs increased in WT mice but not in RES mice. *P < 0.05 (n = 4). (**D**) Bone marrow cells from GFP-expressing mice were transplanted into WT mice. 7 and 14 days after MI, immunohistochemical staining for PECAM (red) was performed, and nuclei were counterstained with TO-PRO-3 (blue). GFP-positive cells (green) represent bone marrow–derived cells that moved into the heart and GFP/PECAM–double-positive cells denote bone marrow–derived endothelial cells. The numbers of GFP– and GFP/PECAM–double-positive cells in the border area (MI group) or LV free wall (sham group) were counted (n = 5–8). Scale bars: 50 μm. (**E**) WT bone marrow cells were transplanted (BMT) into RES mice, MI was induced, and the mice were treated with EPO or saline (control). FS, the number of vessels, and the ratio of vessels to cardiomyocytes in the border area are shown (n = 8).

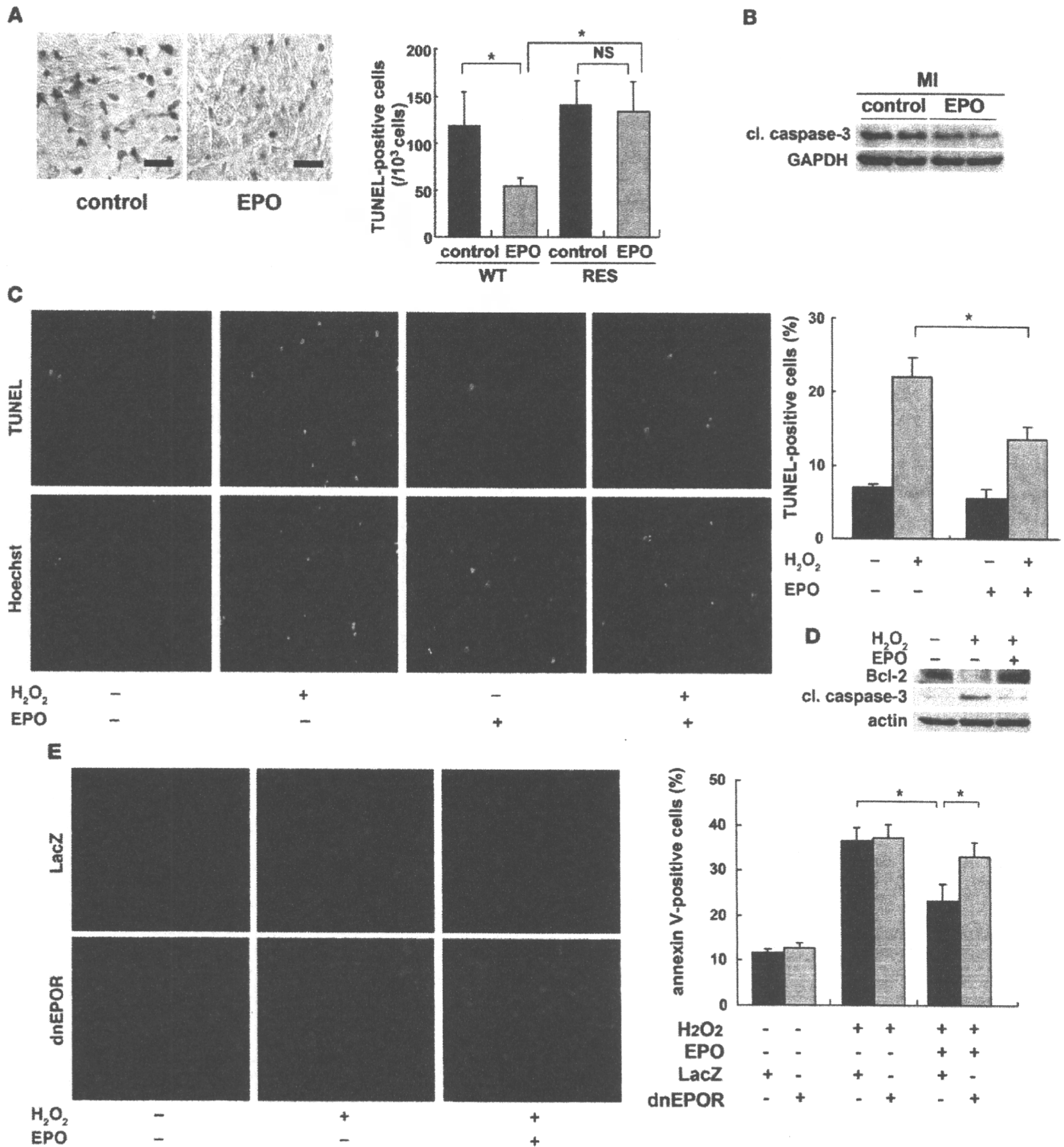

Figure 3

EPO inhibits cardiomyocyte apoptosis in infarcted hearts. (**A**) TUNEL staining (brown) of infarcted hearts from WT mice 24 hours after ligation. Scale bars: 100 μm. The number of TUNEL-positive cardiomyocytes in the border area was counted. $^*P < 0.01$ ($n = 10$). (**B**) Representative Western blots of cleaved caspase-3 (cl. caspase-3) protein in the heart 24 hours after MI are shown ($n = 4$). (**C**) Detection of apoptotic cardiomyocytes using FITC-labeled TUNEL staining (green). Nuclei were counterstained with Hoechst 33258 (blue). The TUNEL-positive cardiomyocytes were counted ($n = 10$). $^*P < 0.05$. (**D**) Samples were pretreated with EPO for 8 hours before H_2O_2 treatment, and the expression of Bcl-2 and cleaved caspase-3 24 hours after H_2O_2 treatment was analyzed by Western blotting. Representative results from 3 experiments are shown. (**E**) Detection of apoptotic cardiomyocytes using Cy-3–labeled annexin V staining (red). Nuclei were counterstained with Hoechst 33258 (blue). Cardiomyocytes were infected with adenoviral vectors encoding dominant negative form of EPOR or LacZ at 10 MOI. The number of annexin V–positive cardiomyocytes was counted ($n = 10$). $^*P < 0.05$.

A

control

EPO

sham day 1 day 7 day 14

vessels/HPF

150 100 50 0

sham day 1 day 7 day 14

vessels/cardiomyocyte

1.6 1.2 0.8 0.4 0.0

sham day 1 day 7 day 14

■ control
▨ EPO

B

control

EPO

sham MI

α-SMA–positive vessels (/mm²)

30 20 10 0

control EPO control EPO

sham MI

C

coronary flow (ml/min)

2 1 0

control EPO control EPO

normal SNP

D

control

EPO

sham MI

positive area (%)

10 5 0

control EPO control EPO

sham MI